

Multifunctional Nanorods for Biomedical Applications

Megan E. Pearce,¹ Jessica B. Melanko,² and Aliasger K. Salem^{1,2,3,4}

Received April 4, 2007; accepted June 15, 2007; published online August 8, 2007

Abstract. Multifunctional nanorods have shown significant potential in a wide range of biomedical applications. Nanorods can be synthesized by a top down or bottom-up approach. The bottom-up approach commonly utilizes a template deposition methodology. A variety of metal segments can easily be incorporated into the nanorods. This permits high degrees of chemical and dimensional control. High aspect-ratio nanorods have a large surface area for functionalization. By varying the metal segments in the nanorods, spatial control over the binding of functional biomolecules that correspond with the unique surface chemistry of the metal segment can be achieved. Functionalized multicomponent nanorods are utilized in applications ranging from multiplexing, protein sensing, glucose sensing, imaging, biomolecule-associated nanocircuits, gene delivery and vaccinations.

KEY WORDS: gene delivery; vaccines; imaging; biomolecule-associated nanocircuits; multifunctional nanorods; multiplexing; protein sensing; glucose sensing; template deposition.

INTRODUCTION

Multifunctional nanorods offer a unique ability to combine a number of essential diagnostic, imaging, delivery and dosage properties. Nanoparticles or nanorods show characteristic size dependent properties with the greatest effects observed in the 1–10-nm size range (1–3). This is due to the large surface area-to-volume ratio of nanoparticles, which increases surface free energy to a point that is comparable to their lattice energy. Nanorods have the capacity for large variations in composition. In addition, their properties have been exploited and designed for specific biological applications by taking advantage of the additional degrees of freedom associated with nanorods in comparison to spherical particles (4). In recent years, there has been an escalation in the development of techniques for synthesis of multicomponent nanorods and subsequent surface functionalization. Multifunctional nanoparticles exhibit characteristic electronic, optical, and catalytic properties significantly different from those of their individual constituent metals. Multifunctional nanoparticles are therefore of considerable interest in the basic and applied biotechnology sciences (5–7). Previous reviews have provided an introduction to multifunctional nanocarriers such as liposomes, micelles, nano-emulsions and polymeric nanoparticles (8), to formation and uses of multisegmented nanorods with respect to applications in magnetics, optics and circuitry (9), or to biological

applications of single component high aspect ratio nanoparticles (10). The following review focuses on the most recent advances in the preparation and use of multifunctional nanorod systems in biomedical applications such as sensing, and drug and gene delivery.

SYNTHESIS

Seed Mediated Synthesis

Nanorods can be synthesized via a “top-down” or “bottom-up” approach by using a hard template or seed mediation method, respectively. Whereas lithographic methods use a “top-down” miniaturization of patterns, the alternative approach of the “bottom-up” construction of objects has been suggested as a means to overcome the limitations of lithography (11). A variety of synthetic chemical methods have been used in the formation of metallic nanoparticles. The most common method involves mild chemical reduction of metal salts in solution phase. The reducing agents used include sodium borohydride (5,12–15), sodium citrate (16), ascorbic acid (17) and less commonly sodium dodecylbenzene sulfonate (18) or hydrazine. These reducing agents are added to the metal ion solutions. Examples of metal ions used include Fe^{2+} , Cu^{2+} , Ag^+ or Pd^{2+} (19). Nanoparticle stabilization can be achieved by surrounding or combining the metal center with sterically bulky materials such as surfactants or polymers. Additionally, synthesis of Ag, Au, Pd or Cu nanoparticles or metal colloids has been achieved by reduction of metallic salts in dry ethanol (3), utilization of air-saturated aqueous solutions of poly (ethylene glycol; PEG; 20), or use of precursors in the form of corresponding mesityl derivatives (1,21).

The chemical synthesis of one-dimensional nanorods and nanowires using a catalyst works by directing the growth of a

¹Department of Biomedical Engineering, College of Engineering, University of Iowa, Iowa City, Iowa 52242, USA.

²Department of Chemical and Biochemical Engineering, College of Engineering, University of Iowa, Iowa City, Iowa 52242, USA.

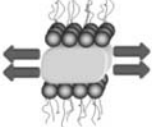


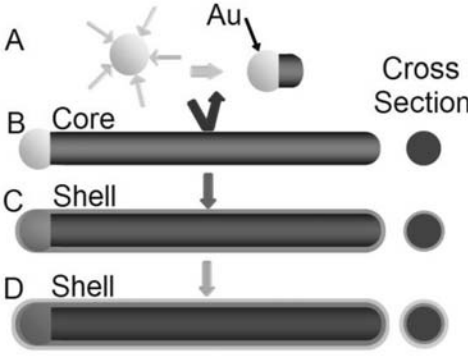
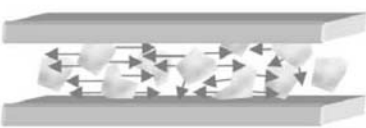
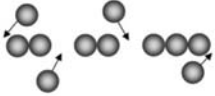
³Division of Pharmaceutics, College of Pharmacy, University of Iowa, Iowa City, Iowa 52242, USA.

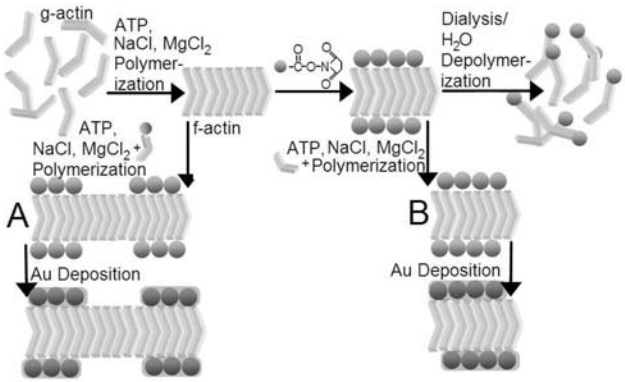
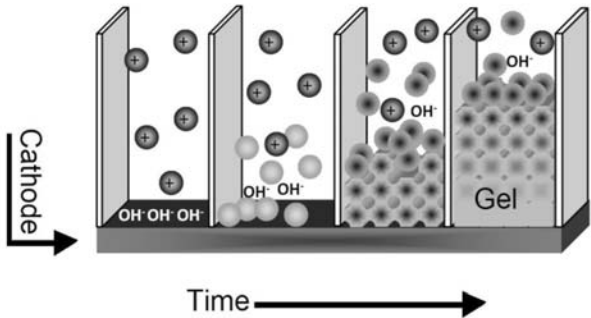
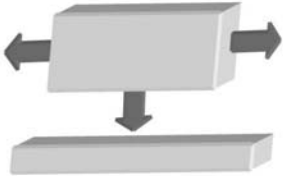
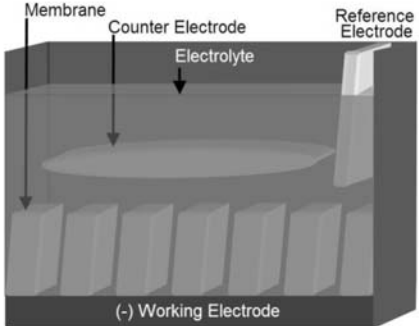
⁴To whom correspondence should be addressed. (e-mail: aliasger-salem@uiowa.edu)

single crystal material through a vapor, liquid, solid (VLS) mechanism. Liquid-forming agents or catalytic agents are required for VLS growth to occur (22). The evolution of a solid from a VLS phase involves two fundamental steps: nucleation and growth. As the concentration of the building

blocks, such as atoms, ions, or molecules of a solid becomes sufficiently high, they aggregate into minute clusters, also known as nuclei, through homogeneous nucleation. If they are given a constant supply of building blocks, these nuclei can function as seeds for further growth of larger structures.

Table I. A Schematic Demonstrating A Large Number of Synthetic Methods, Including Chemical Synthesis (Bottom-up) and Deposition (Top-down) for Forming Single and Multi-functional Nanorods

Method of Synthesis	Proposed Mechanism	Description
Seed-Capping		Growth occurs via kinetic control provided by a capping agent Adapted from reference (15, 124)
VLS Process		Growth occurs through confinement by a liquid droplet as in the vapor-liquid-solid process Adapted from reference (22)
Solid Controlled Growth		Growth is dictated by the anisotropic crystallographic structure of a solid. Adapted from reference (124)
Chemical Vapor Deposition		A) Gaseous reactants catalytically decompose on the surface of a gold nanoparticle, which leads to nucleation and directed nanowire growth. B) One-dimensional growth is maintained as reactant decomposition on the gold catalyst is highly favored. C) Homogeneous reactant decomposition on the nanowire surface forming a uniform shell. D) Repeated modulation forms multiple shells. Adapted from reference (125)
Template		Nanorod/nanowire growth is directed through the use of a template. The hard template can be prepared from a wide variety of materials. Adapted from reference (124)
Self-Assembly		Self-assembly of a one-dimensional nanostructure. Adapted from reference (124)

<p>Biomolecular Template Synthesis</p>		<p>One example of how biological molecules can be utilized to achieve formation of metallic nanowires: The assembly of actin-based Au nanowires. Specific patterning can be achieved with this method. Adapted from reference (11).</p>
<p>Electro-chemically Induced sol-gel process</p>		<p>Sol-gel processes include the hydrolysis of precursor molecules to obtain a suspension of colloidal particles (the sol) and then condensation of sol particles to yield a gel. Precursors can be either organic metal alkoxides in organic solvents or inorganic salts in aqueous media (26). Sol-gel synthesis can be processed in nanoporous template membranes to obtain nanowires, tubules, and fibrils of a variety of inorganic materials. Adapted from reference (42).</p>
<p>Electrodeposition</p>		<p>In this electrochemical method, a thin conducting metal film is first coated on one side of the porous membrane to serve as the cathode for electroplating. Both AC and DC electrodeposition are used for filling the pores (26).</p>
<p>Size-reduction</p>		<p>Size reduction of a one-dimensional microstructure. Adapted from reference (124)</p>

The formation of a crystal requires a reversible pathway between the building blocks on the solid surface and those in the liquid phase. These conditions allow the building blocks to easily adopt the appropriate positions necessary for developing the long-range-ordered, crystalline lattice. In addition, the building blocks need to be supplied at a well-

controlled rate in order to obtain crystals with a homogenous composition and uniform morphology. The catalyst defines the diameter of the nanorods and preferentially directs the addition of the reactant to the end of the growing nanorod (Table I). The process has been compared to a polymerization addition of monomers to a growing polymer chain (23).

More challenging has been the development of a simple chemical synthetic approach to produce multicomponent nanoparticles. A few studies have reported formation of bimetallic nanostructures through chemical synthesis. For example, Jin and Dong (24) have described a simple method for preparing novel Ag–Au bimetallic colloids with hollow interiors and bearing nanospikes by seeding with citrate-reduced silver nanoparticles. Dumbbell-shaped Au–Ag core-shell nanorods were also produced using the same method with gold nanorods substituted as the seeds under alkaline conditions (Fig. 1; 5,25). The synthesis of one-dimensional nanostructures such as nanowires is dependent on constraining the growth of the material in two directions to within a few nanometers and permitting growth in the third direction. The key to achieving one-dimensional growth in materials, where atomic bonding is relatively isotropic, is to break the symmetry during the growth rather than simply arresting growth at an early stage. While this approach is relatively straightforward for single component materials, it becomes more challenging for multi-component materials with defined stoichiometries (26).

Mechanical Synthesis

A common method for generating multicomponent metallic nanowires and nanorods is template-directed synthesis that involves either chemical or electrochemical depositions (27). Template deposition yields a monodisperse suspension of individual particles due to the uniformity and density of the template pores. Each nanorod can have different metal segments along the nanowire (Fig. 2). Each segment can then be

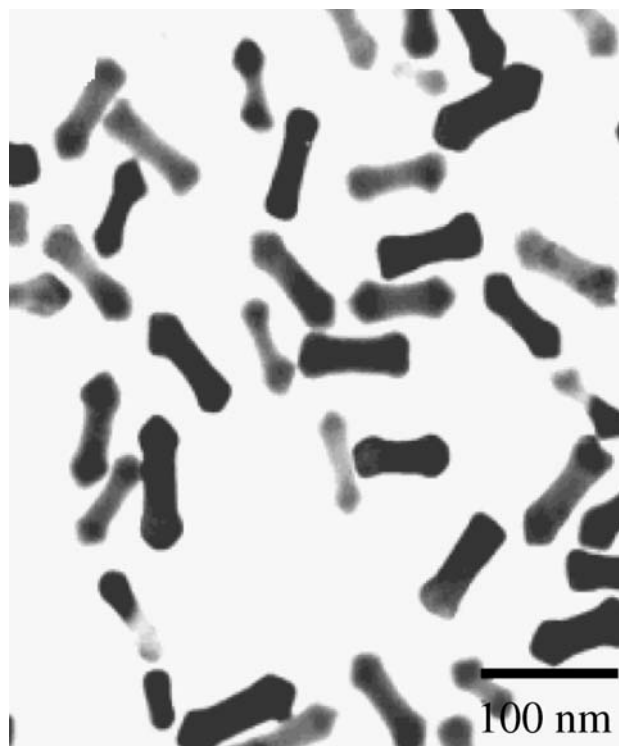


Fig. 1. TEM image of dumbbell shaped Au/Ag nanoparticles. The contrast indicates the core-shell structure, with the bright segments indicating silver. Reprinted with permission from (5). © American Chemical Society (2004).

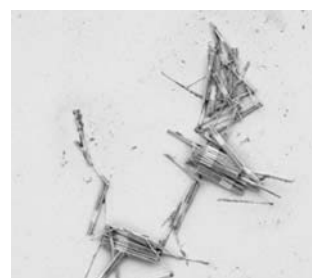


Fig. 2. SEM image showing Ni/Au/Ni nanowires assembly by His₆-ELP-His₆ biopolymers. Reprinted with permission from (112). © Institute of Physics (2006).

derivatized with metal-specific chemistries (4). This method is also available for nanotube and core-shell nanorod synthesis.

Template-based methods utilize either hard templates or soft templates. The hard templates include inorganic mesoporous materials such as anodic aluminum oxides, zeolites, mesoporous polymer membranes, block copolymers, carbon nanotubes, and glass, amongst others. Soft templates commonly refer to surfactant assemblies such as monolayers, liquid crystals, vesicles and micelles (28). The terms template-free or chemical template method are used to describe these methods (26).

A number of materials have shown potential as templates for the fabrication of nanorods, nanotubes and nanowires. However, ion-track-etched membranes and anodic aluminum oxide templates are the most regularly used materials. These items include alumina and polycarbonate filtration membranes obtainable through commercial sources (29), as well as laboratory-made lithographic and anodized alumina templates, which are formed using commercially available aluminum sheets (30,31). Another advantage of hard templates is that during synthesis, precise positions and dimensions of the various constituents of the rods or wires can be manipulated on a very large scale (28,32). For instance, alumina templates have pore densities in the range of 10^{10} – 10^{11} pores·cm⁻² (30). Electrochemical template synthesis has produced both single and multi-component nanowires with diameters as small as a few nanometers and as large as one micron (4). To date, the major drawback of hard template synthesis is the limited thickness of the template membrane. For example, commercial alumina has a thickness of 50–60 μm (30).

Multi-component nanorods are typically prepared by taking a porous template, such as an alumina filtration membrane, and coating one side with a metal film to act as the working electrode. The open side of the template is then immersed in the desired plating solution for electrodeposition. The nanowire length is dependent upon the current passed. Once the desired length has been deposited, the plating solution can be changed and plating may be resumed to produce particles with segments of known length of various specific metals. It is possible to produce large arrays of segmented wires with complex striping patterns along the length of the wires. The electrodeposition process can be computer controlled for simultaneous synthesis of multiple striping patterns in different membranes (30). Recent modifications to the electroplating process have been reported which may increase the reproducibility and monodispersity of rod samples by facilitating the mass transport of ions and gasses through the pores of the membrane. The modifications

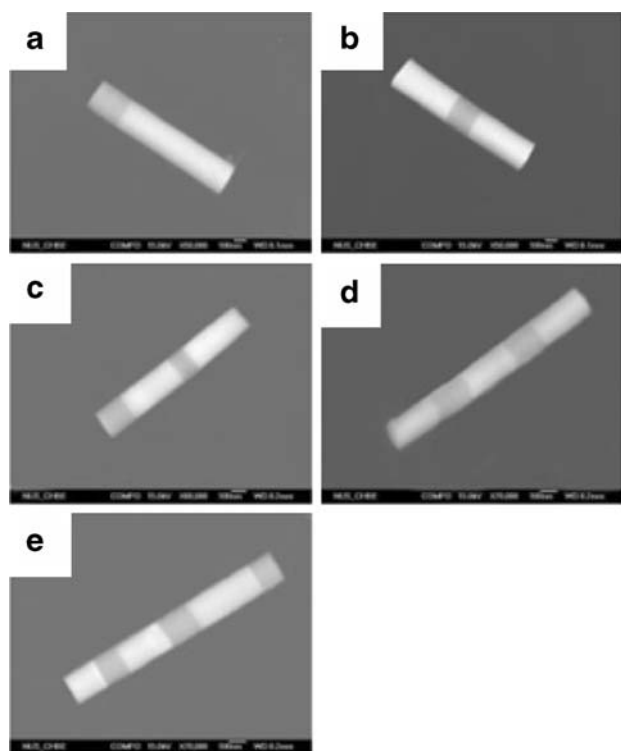


Fig. 3. FSEM images of **a** Pt-Ru, **b** Pt-Ru-Pt, **c** Pt-Ru-Pt-Ru, **d** Pt-Ru-Pt-Ru-Pt, **e** Pt-Ru-Pt-Ru-Pt-Ru nanorods with a 200-nm diameter. Reprinted with permission from (38). John Wiley & Sons, Inc. (2005).

include (1) electroplating within an ultrasonication bath, and (2) controlling the temperature via a recirculating temperature bath (33).

A variety of metal segments can easily be incorporated into the nanowires. Nanorods or nanowires have been prepared with Au, Ag, CdSe, Co, Cu, Ni, Pd, Pt, Ru and Sn segments containing either bimetallic or ternary configurations (Figs. 3 and 4; 30,31,33–39). These synthetic methods permit high degrees of chemical and dimensional control and allow for the formation of useful nanoparticulate systems with a wide variety of biological applications.

A combination of electrochemical methods can also be used to grow bimetallic nanowires. Walter *et al.* describe a complimentary method for preparing long bimetallic nanowires that are compositionally modulated along the axis of the nanowire. The method was described as the “wiring” of two metals. This process utilizes particles of one metal and nanowires of a second. The method is a combination of “slow growth” and nanowire growth, both of which are forms of electrochemical deposition. The beaded bimetallic nanowires were manufactured up to one millimeter in length and in parallel arrays (40).

In addition to chemical and electrochemical deposition, nanowires can also be created via non-electrochemical deposition, sol-gel deposition and biomolecule deposition.

Sol-gel processing has progressed into a useful and broad-spectrum means of preparing highly stoichiometric nanocrystalline materials, especially those consisting of multicomponent oxides. Sol-gel processing involves the hydrolysis of a solution of precursor molecules to first obtain a suspension of colloidal particles (the sol) followed by con-

densation of sol particles to produce a gel (41,42). Precursors may be either organic metal alkoxides in organic solvents or inorganic salts in aqueous media. Each precursor can have different reactivities, hydrolysis and condensation rates, and is able to form nanoclusters of its specific metal or metal oxide, yielding complexes of multiple oxide phases, instead of a single phase complex oxide. This property is advantageous when pursuing multiple surface functionalities (26).

The utilization of biological components for the formation of various inorganic nanorods has also been reported. One of the earliest noted biological templated nanowire synthesis involved metallization of double-stranded DNA between two electrodes to form a conductive silver nanowire. Specifically, complementary single-stranded DNA was used to bridge a 12- μm gap between two gold electrodes, which was then coated with silver via a deposition and enhancement process in order to form 12 μm long 100 nm-wide conductive silver wires (43,44).

Additional examples include Ferritin, which contains a 5 nm diameter ferric oxide core that can be converted to a template upon reduction of the Fe_2O_3 interior. Once the core material has been removed, the channel can be remineralized with various inorganic oxides, sulfides or selenides, such as CdS, CdSe, FeS or MnO (11,45–48). Diphenylalanine β -amyloid short-chain peptides form nanotubes which have been used as templates for growing silver nanowires. The tubes were added to a boiling ionic silver solution, and the silver was subsequently reduced with citric acid to ensure a consistent assembly of the silver nanowires. The peptide template was removed via enzymatic degradation with proteinase K. Analysis of the nanorods showed an 80–90% yield of metal assemblies within the tubes (11,49). Another protein, α -Synuclein, can self-assemble into hollow tubes through β -sheet formation *in vitro*. Fibrillization is enhanced by exposure to various metal ions. The chemicals used in the metallization process were silver nitrate (AgNO_3) potassium tetrachloroplatinate (K_2PtCl_4) and sodium borohydride (NaBH_4). During the metallization process, the cations react with the aminoacyl side chains of the protein at basic pH. The average diameter of the resultant Ag and Pt nanowires was in the range of 40–50 nm, with lengths varying between 500 nm and 1 μm (50).

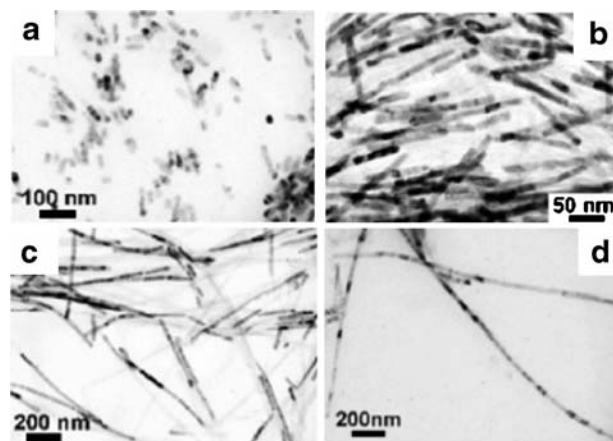


Fig. 4. CdSe nanorods and wires after **a** one template wetting cycle, **b** two template wetting cycle, **c** three template wetting cycle, **d** four template wetting cycles. Reprinted with permission from (122). American Chemical Society (2006).

Peptide assisted nanorod synthesis can also be achieved by the specific assembly of protein subunits into template structures (Table I). These templates can then pattern the generated metal nanowires. The f-actin filament has been utilized as a soft template for the formation of gold nanowires. The filament was covalently modified with 1.4 nm gold nanoparticles (Au NP) which had been functionalized with single *N*-hydroxysuccinimidyl ester groups. Magnesium (2+) and Sodium (1+), which were used to assemble the g-actin monomer units into the filament, were removed upon dialysis of the ATP. This reaction led to filament separation and the formation of gold nanoparticle-functionalized g-actin subunits. The gold nanoparticle-functionalized g-actin subunits were then used as adaptable building blocks for the Magnesium–Sodium–ATP-induced polymerization of the functionalized monomers to generate the Au NP-functionalized filaments of a pre-designed pattern. Electroless catalytic gold deposition on the gold nanoparticle-functionalized f-actin filament produced one to 3- μ m-long gold wires. The nanorod height, which was dependent on the duration of gold deposition ranged from 80–150 nm. The ability to sequentially polymerize the actin filament on the gold-actin wire allowed for patterning. Either actin/Au-wire/actin filaments or inverse Au-wire/actin/Au-wire patterned filaments were generated (11).

Functionalization

A major challenge in synthetic nanotechnology is to not only customize the size, shape and composition, but also to optimize the functionality of the nanoparticles (1). High aspect-ratio nanoparticles have a large surface area for functionalization. When multiple functionalities are introduced, they can be located in optimal positions, depending on their roles, i.e. targeting, tracking or transporting. This avoids molecular interference due to randomly distributed groups, which could lead to malfunction of the system (51). The introduction of different metals allows for the selective functionalization of portions of the nanoparticles (52). For many nano-systems, multifunctionalization can increase specificity of action as well as solubility (53), and compared with monometallic nanoparticles, some bimetallic alloy nanoparticles with a core-shell structure have been reported to exhibit higher catalytic activity (54–56). In order to achieve successful functionalization, the nanowires must be cleaned and isolated, and each functionalization reaction must correspond with the unique surface chemistry of the metal. For instance, gold wires are most often functionalized with thiols, while nickel is most often functionalized with carboxylic acids, which bind to the native oxide layer on the metal (57).

A multifunctional arrangement can also be achieved with nanotubes. The hollow structure allows for two different surfaces which can be autonomously modified with distinct functional groups using a template synthetic method similar to that of nanorods and wires (51). This arrangement possesses the additional function of molecular carrier, as nanotubes have hollow spaces which may be filled with species ranging in size from large proteins to small molecules (58).

Though surface polymeric functionalization is by far the most common means to nanorod specificity, Mbindyo *et al.* demonstrated that internal polymeric incorporation is also a possibility for multifunctional arrangements. Striped nano-

wires incorporated 16-mercaptohexadecanoic acid polymer segments sandwiched between the metallic segments. An electrodeposition method with a track etched polycarbonate membrane that was coated with a 100 nm layer of gold was utilized. Monolayers of 16-mercaptohexadecanoic acid were assembled at the tip of the nanowires followed by electroless plating to introduce metal caps on top of the monolayer (59).

Similarly, Hernández *et al.* reported the synthesis of segmented Au–polypyrrole–Au nanowires. This metal-polymer hybrid synthesis was taken a step further by incorporating proteins in the polymer component. Protein incorporation is an improved step towards biocompatible sensors and assemblies. The nanowires were made using anodic alumina templates in aqueous phosphate-buffered saline solution by either constant potential or potential cycling electrochemical methods. The choice of electrochemical method had an influence on the morphology, appearance, and adhesion of polypyrrole films (60). The nanowires were 300 nm in diameter and a few micrometers long. Following synthesis, the nanowires were analyzed with respect to various growth parameters, such as pH, monomer concentration and electrochemical method of growth. The choice of electrochemical method leads to differences in kinetic and mechanical behavior of the nanowires that are relevant to their use in sensors and self-assembling structures. The proteins avidin and streptavidin were introduced into the nanowires by entrapment during polypyrrole polymerization. The biotin–avidin association was used to monitor the protein incorporation and accessibility in the conducting polymer segments of the nanowires as a function of the conditions of synthesis (61).

Single-crystal nanorods, wires and tubes can be rendered multifunctional depending on the means of functionalization. For example, Banerjee *et al.* selectively functionalized nanotubes to achieve location specific protein functionalities. This configuration could be important in the formation of nano-devices, as selective protein functionalization may be more suitable than DNA due to the increased quantity of highly selective interactions toward their complementary proteins (58,62–66). We have shown that selective functionalization of multi-component nanorods can be achieved using metal-specific chemistries. For example, with Au–Ni bimetallic nanorods, thiol moieties can be used to bind biotin (67,68), proteins (69) or cell targeting ligands (36) to the Au segment. Carboxylic acid moieties can be used to bind DNA to the Ni portion or can be used to block the surface of the central segment of tri-component nanowires so that only the tips are functionalized (36,68). Such end-functionalized multi-component nanorods have potential for use in micro-switch arrays or for building hierarchical structures (67,68). Several groups have successfully achieved various selective functionalization of single and bimetallic nanoparticles with a variety of arrangements. Table II illustrates a number of functionalization strategies on selective gold, nickel, or platinum segmented nanorods.

BIOLOGICAL APPLICATIONS

Protein–protein interactions, enzymatic conversions, and single molecule stochastic behavior take place at the nanoscale. Therefore, nanoscale based measurements allow reinterpretation of observations from large-scale or bulk techniques in order to gain new insight into molecular events that have

cellular, tissue, and organismal phenotypic manifestations (70). A wide variety of nanorods and wires have been utilized in biological applications, such as construct of electronic or sensor device configurations. The synthesis of smart nanotubes, rods and wires which are able to recognize specific complementary molecules and perform specific functions has become increasingly important. With increased specificity we can continue to derive novel devices and procedures by guiding those nano-sized building blocks to the correct

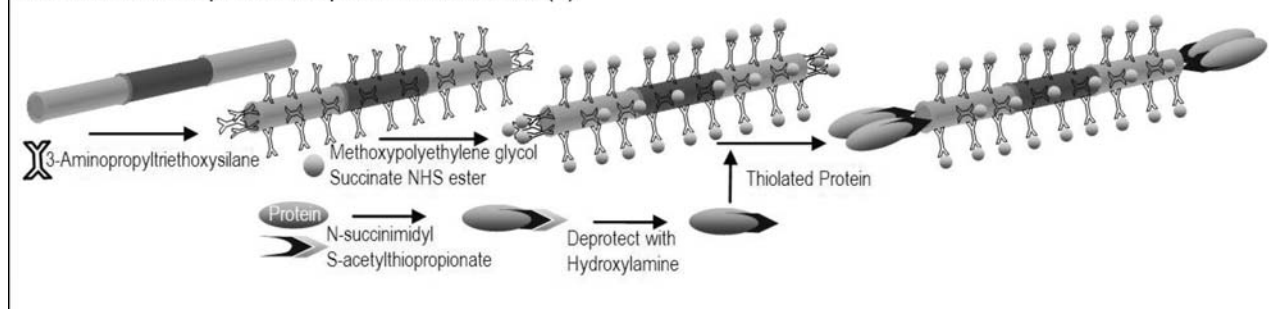
position through molecular recognitions and self-assemblies (66–68).

Multiplexing

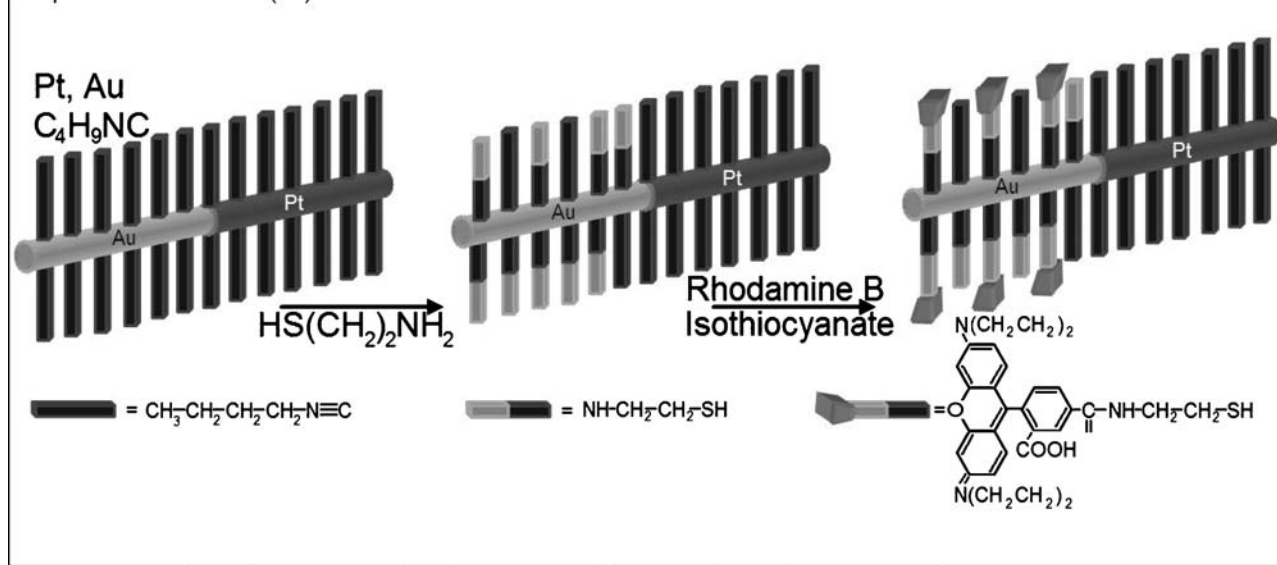
Driven by demands for cost-efficiency, there is an ever-increasing need to quantify a large number of species from minute sample volumes and to find disease biomarkers or genetic mutations in bioanalysis. Multiplexing gives research-

Table II. Examples of Selective Functionalization of Multisegmented Nanowires for Use in Biomedical Applications and/or Self Assembly

Thiolated KE2 Antibody Selectively Bound to the Au Segments on Au/Ni/Au Nanowires The nanowires were fabricated within alumina templates. Adapted from reference (4)

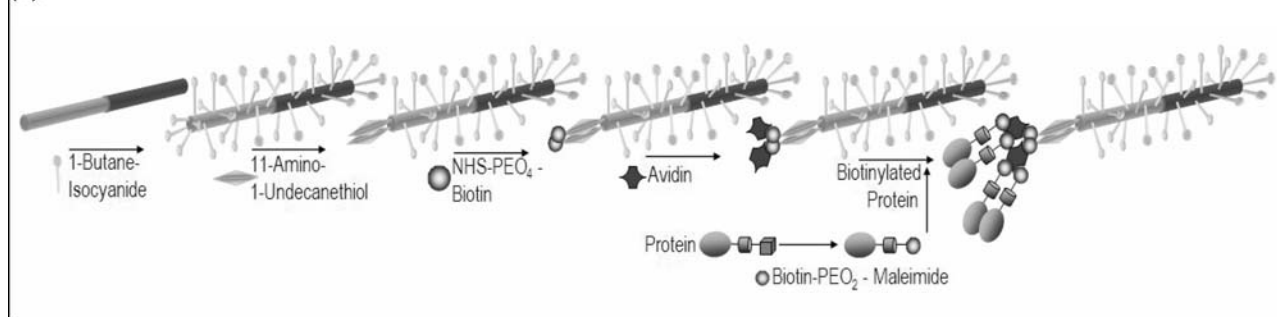


Orthogonal self assembly on gold and platinum nanorods. These rods also have the capability to self-assemble. Adapted from reference (33)

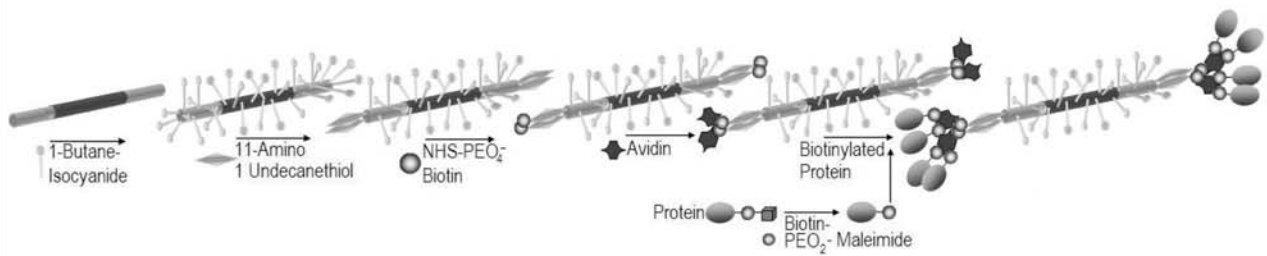


Biotinylated ActA-Cys Bound to the Au Segments on Au/Pt Nanowires. Adapted from reference

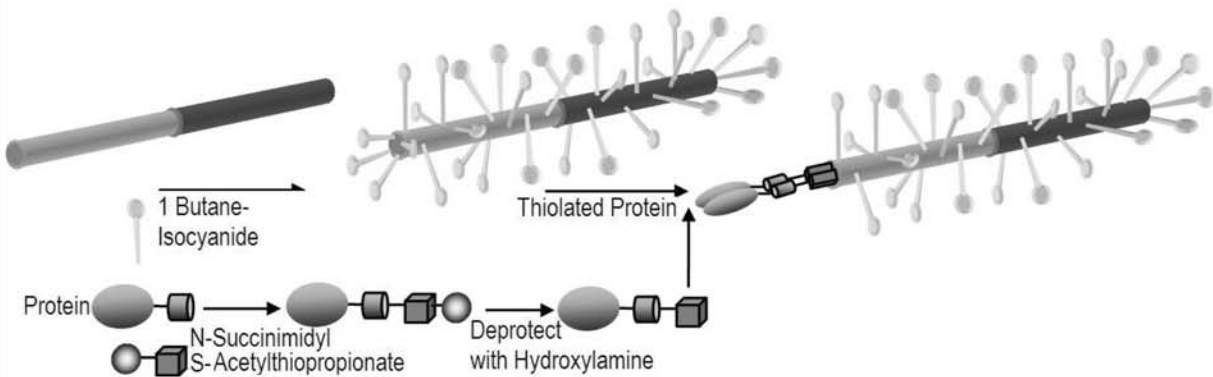
(4).



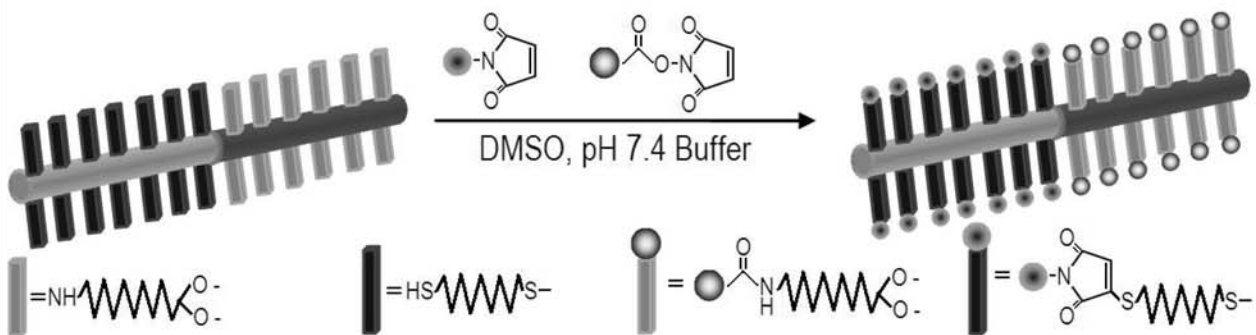
Biotinylated ActA-NH2 Selectively Bound to the Au Segments on Au/Pt/Au Nanowires. Adapted from reference (4).



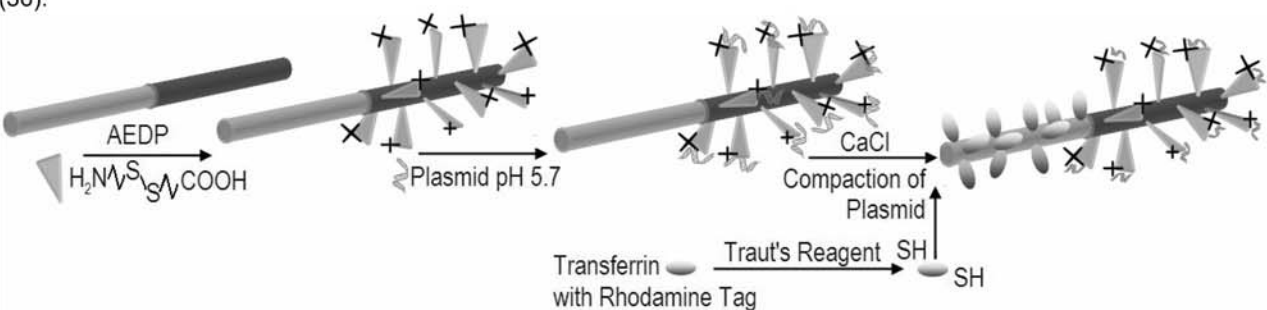
Thiolated ActA-NH2 Protein Selectively Bound to the Au Segments on Au/Pt Nanowires. Adapted from reference (4).



Selective protein adsorption on a gold-nickel nanowire Adapted from reference (10).



The procedure begins with 3-[(2-aminoethyl) dithio] propionic acid (AEDP) linker incubation. Adapted from reference (36).



ers a way to perform thousands of simultaneous assays (35). There are numerous novel approaches to multiplexing involving multicomponent nanorods containing a bimetallic striped pattern. Current assays for determining DNA sequence rely on spatial addressing. With nanoparticles, biomolecule identity is optically programmed in the particles themselves. This is frequently a fluorescent or Raman scattering signature (39,71–76). Encoded particles are functionalized with the objective biomolecule and then several particle patterns are blended to generate a solution-based analogue of a microarray. Solution arrays promise greater biorecognition efficiencies due to improved diffusion and flexibility (30). Keating *et al.* reported the use of striped metal nanowires as bar-coded substrates for multiplexing. The bar-coded nanorods demonstrated the ability to be functionalized for detection of specific analytes. The experiment included a sandwich assay in which a nanorod, functionalized with a biomolecule, bound an analyte from solution. A fluorescently tagged secondary antibody or oligonucleotide was also added for detection. Figures 5 and 6 show the approach used for three simultaneous sandwich immunoassays. It was critical for the fluorophore to be located sufficiently far from the metal surface so that quenching may be avoided. This is especially important for those particles functionalized with small moieties, such as oligonucleotides (30).

A similar approach using fluorescence to designate analyte presence and barcode pattern to ascertain analyte identity was used by Tok *et al.* The degree of binding with antibody-conjugated multi-stripped metallic nanowires and a fluorophore-tagged antigen target was investigated. The purpose of the detection was to enable rapid and sensitive single and multiplex immunoassays for biowarfare agent stimulants. Hybridization and capture kinetics of the objective analyte in solution favored the nanowires over standard fixed array-based formats. A ferromagnetic Ni component was incorporated in order to facilitate magnetic field manipulation of the nanoparticles. Tests were performed with a set of three nonpathogenic stimulants: *Bacillus globigii* spores to simulate *Bacillus anthracis* and other bacterial species, RNA MS2 bacteriophage to simulate *Variola* (the virus for smallpox) and other pathogenic viruses, and

ovalbumin protein to simulate protein toxins such as ricin or botulinum toxin. The samples demonstrated successful size variant capabilities, ranging from 2 μm to 2 nm (77).

These techniques rely on spectrometric encoding with distinct spatially embedded barcodes, which overcome many of the problems associated with conventional multiplexing planar arrays. With the available optical resolution, the number of possible readable “barcodes” that comprise two metals with a coding length of 6.5 nm is limited to 4160. In contrast, for three-metal barcodes, 8.0×10^5 distinctive striping patterns are possible (11). However, the efficiency of these striped barcodes is still limited by the need for coupling chemistries and single batch synthesis. Pregibon *et al.* have produced two-dimensional multifunctional particles capable of analyte encoding and target capture. Their synthesis uses two polymers, one containing fluorescent dye and the other an acrylate-modified probe. Streams of each monomer were flowed adjacently down a microfluidic channel while using a variation of continuous flow lithography to polymerize the particles. As a result, particles with amalgamated fluorescent, graphically encoded regions and probe-loaded regions were synthesized in one step. Each particle produced was an extruded two-dimensional shape with a variable morphology determined by a photomask which is inserted into the field-stop position of the microscope and whose chemistry is determined by the content of the co-flowing monomer streams. The coding system is a simple series of dots that can generate over a million codes. Particles were designed to be digitally read along five lanes, with alignment indicators used to identify the code position and direction regardless of particle orientation. A variety of channel designs was used to generate particles bearing a single probe region, multiple probe regions, and probe-region gradients (Fig. 7). The system’s multiplexing capabilities were tested using acrylate-modified oligonucleotide probes for sequence detection. The largest benefit of this approach is the reproducibility, high throughput detection and direct incorporation of probes into the encoded particle. This system has the potential for incorporation of magnetic nanoparticles within the gradient, which could produce a temperature variation along the particle when stimulated in an oscillating magnetic field (78).

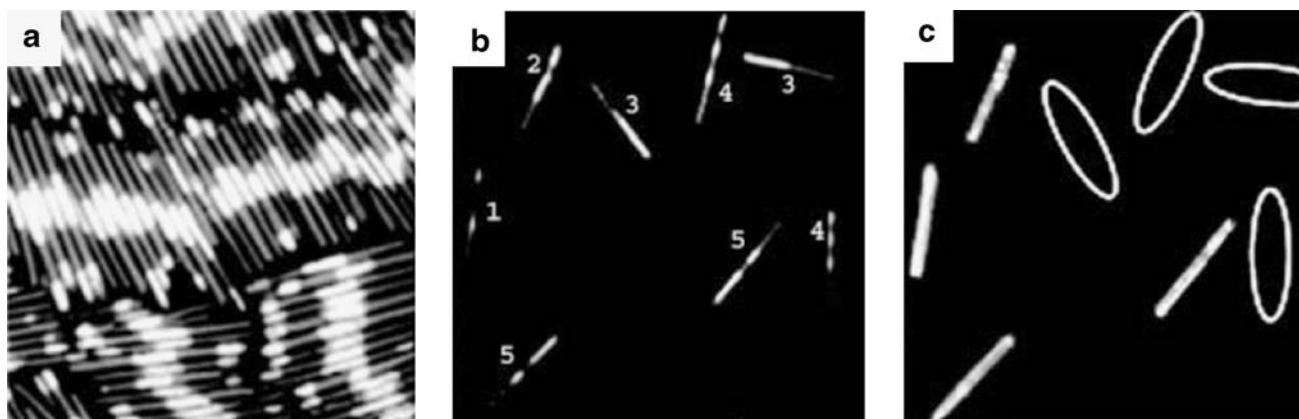


Fig. 5. **a** Close-packed array of 300 nm \times 6 μm , Ag–Au–Au–Ag–Ag–Au–Au–Au striped metal rods. **b** Reflectivity image of an assortment of antibody-functionalized rods used in a multiplex sandwich immunoassay. **c** Fluorescence image for the rods from **b**. The ellipses denote the absence of fluorescence signal from particles lacking a bound analyte. Reprinted with permission from (30). © John Wiley & Sons, Inc. (2003).

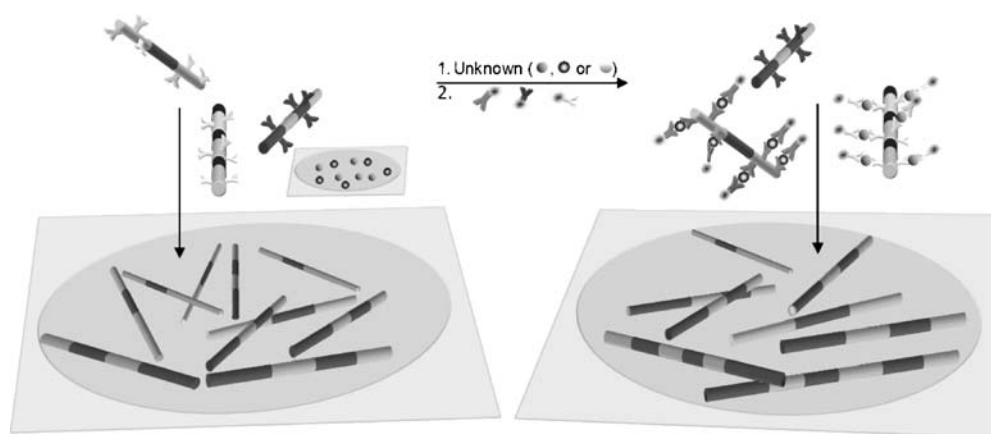


Fig. 6. A schematic of a bimetallic barcode multiplexing experiment. The *left diagram* illustrates how reflectivity can be used to identify and quantify particles. The *right diagram* demonstrates how a measure of reflectivity and fluorescence intensity is performed for each particle. Diagram is adapted from reference (30).

Protein Sensing and Absorption

Nanosensors based on semiconductor nanostructures, such as carbon nanotubes, nanowires, and nanorods, have recently attracted considerable attention for detecting a variety of protein molecules (79,80). Successful application of a protein sensor requires specific protein binding capabilities. Similar to the multiplexing technique, many groups have incorporated multifunctionalizations for location and type-specific protein attachment. However, specifically attaching proteins to individual segments of nanowires in order to achieve differential functionalization is particularly challenging because proteins tend to bind to most surfaces (4).

Meyer and colleagues have reported successful selective protein adsorption onto multicomponent nanowires. Two-component gold–nickel nanowires (10–25 μm long; 200 nm diameter) were selectively functionalized with alkylterminated monolayers on nickel and hexa (ethylene glycol) (EG_6)-terminated monolayers on gold. Selective functionalization was achieved using metal specific gold–thiol and nickel–carboxylic acid interactions. Alexa Fluor[®] 594 goat antimouse IgG fluorescently tagged antibody proteins preferentially adsorbed to the methyl terminated nickel surfaces, but the EG_6 -terminated gold wires resisted protein adherence. The results demonstrated that multicomponent nanostructures can be modified at the molecular level to yield materials on which proteins adsorb selectively in specific regions (57,81).

Sheu *et al.* achieved protein binding and subsequent electrical detection through a multicomponent system consisting of gold nanoparticles bound to *N*-(2-Aminoethyl)-3-aminopropyl-trimethoxysilane (AEAPTMS)-pretreated silicon nanowires. The silicon nanowires were fabricated by scanning probe lithography and wet etching methods. Conductance changes were measured in order to monitor the reaction between the gold particles and the nanowire surface. A thiol-engineered enzyme, KSI-126C, was then bound to the gold nanoparticles on the surface of the wires. Shifts in turn-on voltage clearly demonstrated the system's effectiveness following the binding of the protein molecules and gold nanoparticles (82). Nanorods that can sense proteins at low concentrations also have potential in a wide variety of applications including glucose sensing.

Glucose Sensing

Currently, over 18 million Americans are living with diabetes. To help control this disease, patients must carefully monitor their blood glucose levels in order to make appropriate food choices or determine the need for insulin injections (83). Given this widespread need for glucose monitoring, the use of functionalized nanotubes and nanorods for glucose sensing is an increasingly researched area. For example, composite electrodes have been constructed by mixing carbon nanotubes with granular Teflon (84). The Teflon acted as a binder, with the carbon nanotubes acting as the conductor. H_2O_2 and NADH redox activity in the Teflon/carbon was observed at potentials significantly lower than those observed with the graphite/Teflon electrodes. The ability for low-potential detection of H_2O_2 and NADH makes the carbon nanotube/Teflon composite electrode appealing for biosensing applications when used in combination with oxidase and dehydrogenase enzymes. Including either glucose oxidase or alcohol dehydrogenase in the composite turned the majority of the electrode into a reservoir for the enzyme. Amperometric sensing of glucose and ethanol was carried out with these electrodes, and signals of up to 2.4 μA were observed. The low-potential detection allowed these carbon nanotube/Teflon composite electrodes to be very selective, and unaffected by common hindrances such as acetaminophen or uric acid at voltages of 0.1–0.2 volts. The multifunctional structure of these electrodes combines the electronic properties of carbon nanotubes with the benefits of bulk electrodes (84).

Another multifunctional nanoparticle that has been used to study amperometric sensing ability is single-walled carbon nanotubes (SWNTs) with non-covalently bound enzymes (85). SWNTs with adsorbed glucose oxidase were drop-dried onto glassy carbon to be used as electrodes in various solutions. When exposed to glucose, large anodic current responses were observed at these electrodes, as would be expected with catalytic oxidation of glucose. Though the glucose oxidase was bound to the carbon nanotubes, the enzymatic activity was not hindered in the binding. When comparing these results to the same electrode with immobilized glucose oxidase only, the system with the SWNT generated a current more than ten

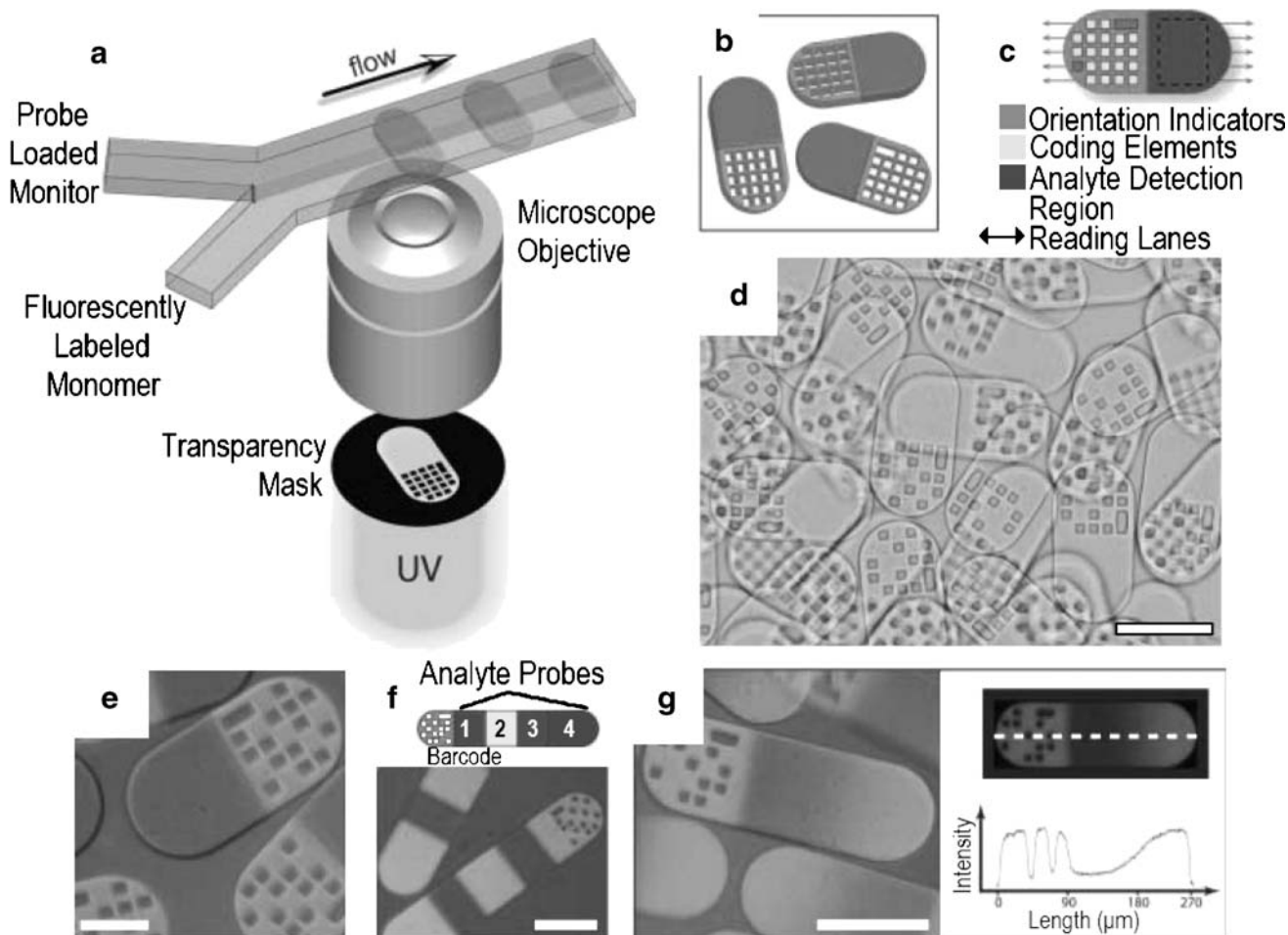


Fig. 7. **a** An illustrative method for synthesis of dot-coded particles via polymerization across two adjacent laminar streams which form single-probe, half-fluorescent particles as depicted in **b**. **c** A representation of specific particle features for encoding and analyte detection. The encoding scheme developed allows for the invention of 2^{20} (1,048,576) unique codes. **d** A differential interference contrast (DIC) image of the particles generated. **e-g** An overlap of fluorescence and DIC images of single- (**e**), multi-, and gradient- (**g**, left) probe encoded particles. *Upper f* is a diagram of multi-probe particles and *right g* is a plot of fluorescent intensity along the center line of a gradient particle. Scale bars designate 100 μm in **d**, **f**, and **g** and 50 μm in **e**. Reprinted with permission from (78) © AAAS (2007).

times greater than the immobilized system. The high conductance and transducing ability of the SWNTs coupled with the high enzyme loading resulted in this significant increase.

In the past ten years, several groups have studied the use of individual semiconducting SWNTs as sensors by incorporating them into field-effect transistors (FETs; 86). A FET is made up of two electrodes, one a source and one a drain, connected by a semiconducting channel. When the appropriate voltage is applied to a gate, current will flow through the channel. A single nanotube biosensor to detect glucose was composed of SWNTs that were formed by chemical vapor deposition. A lithographically patterned electrode was then attached to each end. Pyrene butanoic acid was used as a coupling agent to immobilize glucose oxidase to the tube. The pyrene binds to the nanotubes through Van der Waals interactions and the carboxylic acid forms an amide bond with the enzyme. Figure 8 shows an idealized schematic picture of the nanotube setup. The strong potential that carbon nanotubes have shown in enhancing glucose sensing should be readily extrapolated to nanorods and nanowires prepared from a range of other materials.

Imaging

When metal is in the form of a colloidal particle, the condition for excitation of a plasmon is shifted as compared to its equivalent bulk material. The absorption spectra of many metallic nanoparticles is characterized by a strong broad absorption band that is absent in the bulk spectra. Gold nanorods can be used as sensors because of the size and shape dependence of their optical properties and the ease by which their surfaces can be modified using biological molecules, such as proteins and DNA, primarily through Au-S bonding (5). Bimetallic nanowires that are compositionally modulated along the axis of the nanowire can form the basis for nanowire optical labels. As a result, multifunctional nanomaterials have considerable potential as units for cancer-specific therapeutic and imaging agents (51). Plasmonic metal nanoparticles have significant potential for applications in chemical and biological sensing because they possess sensitive spectral responses to the local environment of the nanoparticle surface. This allows for easy monitoring of the light signal due to their strong scattering or absorption

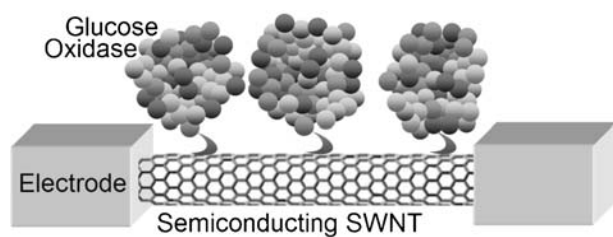


Fig. 8. Schematic of two electrodes connecting a semiconducting nanotube with glucose oxidase immobilized on its surface. Adapted from reference (86).

(32,35,87). By incorporating numerous segments within one particle, they are able to serve as multi-wavelength fluorescent tags. The only requirement for this technique is that the nanorods emit bright light at room temperature (88). The use of ternary compounds (a–b–c) will institute band gap energies between the two binary constituents (a–b) and (b–c). Thus, by controlling the composition of the metals one could design the band gap of an active region. Svensson *et al.* presented a GaAsP segment with a direct band gap into a GaP nanowire, which innately has an indirect band gap (Fig. 9). The segment was then able to function as an optically active segment. The heterostructure GaP/GaAs_{1-x}P_x/GaP metallic nanowires were produced by metal organic vapor phase epitaxy. The wires were approximately 2.8 μm in length with a midline width of around 60 nm. A photoluminescence system was utilized to demonstrate single nanowires emitting different wavelengths at room temperature. Further analysis showed that when the segments are grown with PH₃ flow in parallel with AsH₃, the spectra are blue shifted, with the shift magnitude dependent on PH₃ flow. The structures would be effective components of optoelectronic devices or tags within biomedical analytical systems (88). Significant effort has been concentrated on the band-edge emission in semiconductor nanostructures (89–96). Lanthanide (Yb³⁺/Er³⁺, Yb³⁺/Tm³⁺, etc.)-doped materials possess unique upconversion fluorescence properties, whose growth may increase these compound's promise for use as an ultrasensitive multicolor biolabel (97–99). Hexagonal NaYF₄ is one of the most efficient visible upconversion host materials. However, accurate control of its crystallinity, morphology, and especially epitaxial growth had not been successfully achieved until recently (100–102). Wang and Li have recently demonstrated the synthesis, downconversion/ upconversion fluorescence, and self-assembly of the anthanide-doped Na(Y_{1.5}Na_{0.5})F₆ (hexagonal NaYF₄) single-crystal nanorods. The straightforward protocol should be applicable to other Na(Ln_{1.5}Na_{0.5})F₆ systems, and together with increased

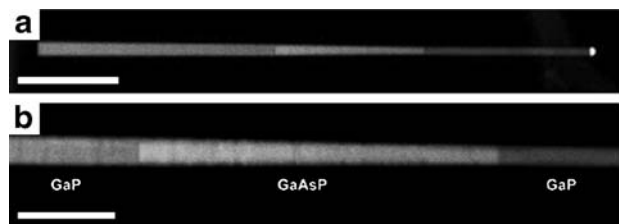


Fig. 9. **a** An image of the GaAsP segment within a GaP nanowire. The wire length is approximately 740 nm. **b** A magnification of the GaAsP segment. The scale bar is approximately 200 nm. Reprinted with permission from (88). © Institute of Physics (2005).

functionalization success, could lead to a highly effective and novel ultrasensitive biolabel for *in vivo* imaging (103).

Biomolecule-Associated Nanocircuits

A significant advantage of nanowires, compared to other low dimensional systems, is that they have two quantum confined directions. This leaves the third dimension unconfined, which is optimal for electrical conduction. This property allows nanowires to be used in applications where electrical conduction rather than tunneling transport is required (26). Cadmium selenide (CdSe) is the most extensively studied compound semiconductor because of the versatile size-tunable properties of its nanostructures (104).

One-dimensional nanowires, specifically, are able to prevent reduction in signal intensities which are innate to higher-dimensional structures. This property of the one-dimensional nanostructures provides a sensing modality for label-free and direct electrical readout when the nanostructure is used as a semiconducting channel of a chemiresistor or field-effect transistor (105,106). This type of label free direct detection is especially advantageous for rapid and real-time monitoring of receptor–ligand interactions with a receptor-modified nanostructure. This is particularly true when the receptor is a biomolecule such as an antibody, DNA, or protein. In the future, this procedure could prove to be critical for accurate clinical diagnosis (106).

Lazarek *et al.* have developed a highly reproducible multicomponent nanorod system with conductance characteristics and possible applications in imaging. Optically active nanostructures were produced that yield devices which are electronically functional at the nanometer scale. This was accomplished via delivery of DNA-modified nanoparticles capable of site-specifically addressing the tips of vertically aligned carbon nanotubes. These then serve as catalysts for the growth of zinc oxide (ZnO) nanorods (Fig. 10). The starting material for the ZnO nanorod growth on carbon nanotube tips are highly ordered multiwalled carbon nanotubes within an aluminum oxide nanopore template. Nitric acid etching introduced carboxylic groups at defect sites, which are located at the tips. The tips can be accessed and linked by the introduction of single-stranded amine-terminated DNA using amide-coupling chemistry in aqueous/

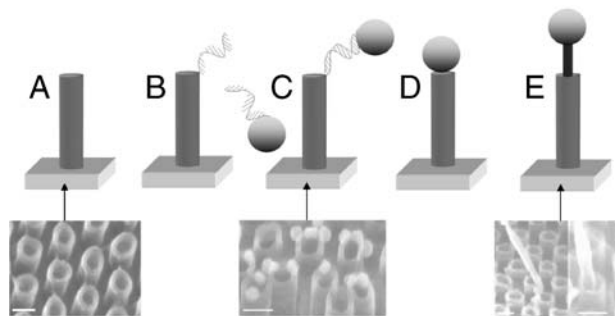


Fig. 10. ZnO–CNT hybrid nanostructures from DNA sequence dependent catalyst placement. SEM images of different ZnO nanorods on top of multiple CNTs are taken at various angles, 30° left panel and 45° right panel, respectively. All SEM scale bars are 50 nm. Reprinted and adapted with permission from (123). © American Institute of Physics (2006).

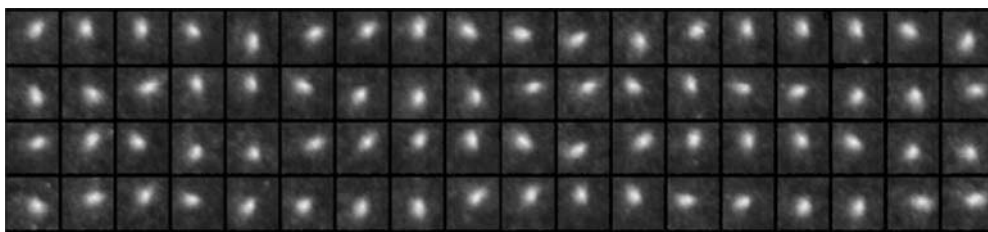


Fig. 11. Sequential images showing the bimetallic nanowire rotating as it is driven by an F_1 -ATPase motor at 2 mM. The F_1 -ATPase motor attaches to the nickel segment of the nanowire. The length from the rod axis to tip is $0.7\ \mu\text{m}$, the rod's rotary rate is 3.7 r.p.s., and the duration between images is 40 ms. Reprinted with permission from (109). © Springer (2006).

organic solvent mixtures. After the conjugation of an amine-terminated DNA strand to the carbon nanotube tips, a complementary second strand was attached to a 20 nm gold particle and hybridized. This ensured that the nanoparticles bound to the carbon nanotube tips. It was noted that some nanotubes exhibited up to three nanoparticles on their tips. The gold nanoparticle-modified carbon nanotubes then underwent chemical-vapor deposition using a VLS growth

process (107). ZnO nanorods developed from the gold nanoparticle catalyst attached to the nanotube tips. The resulting ZnO-carbon nanotube structures had a gold contact at the ZnO end. The uniform length, vertical alignment of the ZnO-carbon nanotube structures, and presence of a gold nanoparticle contact at the ZnO tip were amenable to electrical characterization with conductive probe atomic force microscopy. Several hundred current-voltage measure-

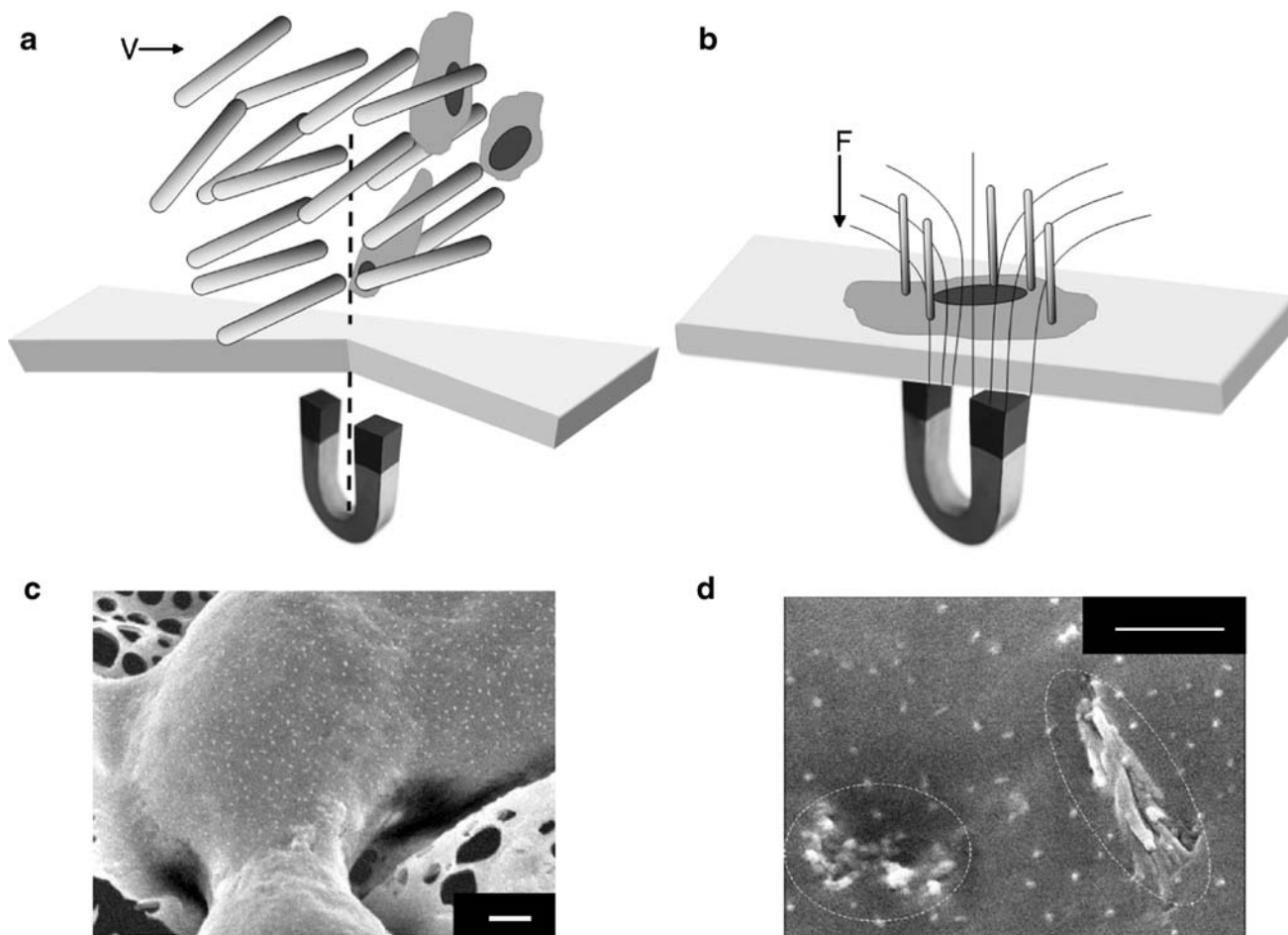


Fig. 12. A two-step protocol for nanotube sparring. **a** A rotating magnetic field drives the Ni-tipped nanotubes to sparring the cells. In the second step, **b** a static field persistently pulls nanotubes into the cells. V indicates the direction of the velocity while F indicates the direction of the magnetic field. The bottom images are SEM micrographs of MCF-7 cells before **c** and after **d** the sparring process. Scale bars in **c** and **d** are $1\ \mu\text{m}$ and $500\ \text{nm}$, respectively. The ovals indicate the location of embedded nanotubes. The small dots on the surface of the cell are microvilli, which exhibit similar densities between the two cells ($15\ \text{microvilli}/\mu\text{m}^2$). Photographs and adapted schemes from reference (110). Reprinted with permission from Macmillan Publishers Ltd. © (2005).

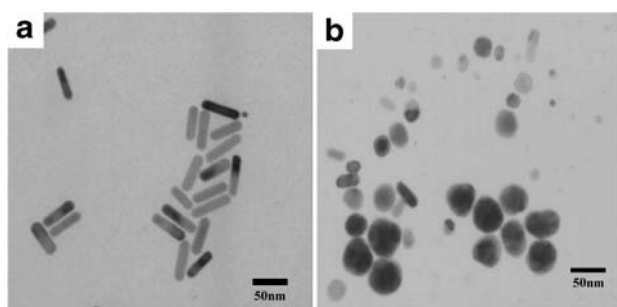


Fig. 13. Typical TEM images of EGFP-GNR conjugates **a** before and **b** after irradiation with laser beam (70 uJ/pulse for 60 s). Reprinted with permission from (112). © Institute of Physics (2006).

ments carried out on the system showed that DNA-directed formation of ZnO-carbon nanotube structures is site specific, size controlled, and also yields a heterojunction that is electronically functional (108).

Future applications in nanocircuitry are not restricted to electrical conductance. Synthesized nanomachinery offers some unique opportunities to harness cellular functions for diagnostic or therapeutic uses. For example, Ren *et al.* have shown that multicomponent nanowires can be assembled with F_1 -ATPase motors in order to form a nano-biohybrid device. These have potential in advanced biosensors and force bioactuators. The F_1 -ATPase mechanism involves an inner γ subunit, which rotates against the surrounding $\alpha_3\beta_3$ subunits during the hydrolysis of ATP in the three catalytic β subunits of the F_1 -ATPase. The reverse rotation of γ subunit in ATP synthase, powered by proton flow, results in ATP synthesis in three β subunits.

Regular application of the F_1 -ATPase motor would be highly dependent on the ability to fabricate and functionalize the propellers for the motor. As a possible solution to this problem, multi-component nanowires were utilized with three segments of Ni/Au/Ni fabricated by electrochemical deposition. The rods were selectively functionalized with thiol modified single-stranded DNA and a biotinylated peptide on the gold and nickel segments, respectively. Attachment of the F_1 -ATPase motor was achieved through the nickel segment of the nanowire via the biotin-streptavidin linkage. Observation of the rotation of the motor-driven propeller (Fig. 11) established the nanowires capability for successful nanoscale assembly and selective functionalization (109). It also highlights the potential of combining biologically active moieties with inorganic nanorods. Such hybrid inorganic-biological nanorod systems have shown significant potential in gene and drug delivery applications.

Multi-functional Nanorods for Gene Delivery

Gene therapy is highly dependent on the ability of the carrier to efficiently deliver the plasmid DNA to the target cells. Cellular uptake of the delivery system is a major barrier confronting these carrier systems. In order to overcome this barrier associated with gene transfection, Cai *et al.* prepared carbon nanotubes with nickel end segments that can be magnetically manipulated (Fig. 12). The carbon nanotubes were grown by plasma-enhanced chemical vapor deposition with ferromagnetic catalyst nickel particles enclosed in the

tips. The delivery of the nanotubes to the cell interior is achieved by using a magnetic field to increase the momentum of the nanoparticles to a point where the tubes can penetrate the cell membrane without significant damage. Splenic B cells, *ex vivo* neurons and transformed mouse B lymphocytes all demonstrated high transduction efficiency, as long as the process was accompanied by (1) nanotubes with plasmids, (2) exposure to a magnetic field and (3) subsequent magnetic response of the nanotubes. Perturbation of the cellular structure was minimal. Even in typically delicate neuronal cells, the cell populations exhibited viability equivalent to the controls. This study focused on plasmid DNA delivery, but potential applications could extend to transportation of other biomolecules such as proteins, peptides or RNA. The process is easily controlled via the magnetic field strength (110,111).

Recently, studies have explored the possibility of developing better control of nanocarriers by applying photon irradiation to trigger biological activity (112). In this way, the carrier would not only deliver the gene to the cell, but also serve as the switch to turn on gene expression. Near-infrared (NIR) irradiation has good therapeutic potential, as it can penetrate deeper into the tissues and would cause less damage when compared to UV-vis irradiation (113,114). For example, EGFP DNA has been conjugated to gold nanorods (EGFP-GNR conjugates). EGFP is the enhanced green fluorescence protein gene, which can be used to track and visually show gene expression both *in vitro* and *in vivo*. To characterize the effects of NIR irradiation, UV-vis spectroscopy, electrophoresis, and transmission electron microscopy were used to reveal the optical and structural properties of the nanorod conjugates before and after laser treatment (Fig. 13). When the EGFP-GNR conjugates were exposed to femto-second NIR irradiation, the gold nanorods changed their shapes and sizes, and released DNA. After EGFP-GNR conjugates were introduced into HeLa cells and irradiated with the NIR source at a dose that did not cause significant lethality, GFP expression was specifically observed in areas locally exposed to laser irradiation. Cell targeting ligands can be utilized to further enhance the efficacy of nanorod mediated gene delivery.

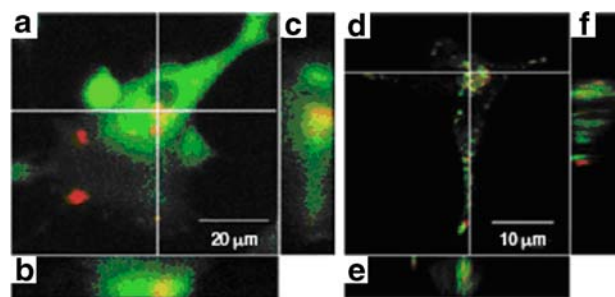


Fig. 14. **a** A live HEK293 cell (red/633 nm, green/543 nm). Rhodamine (633 nm) identifies the subcellular location of the nanorods whilst GFP expression (543 nm) provides confirmation of transfection. **b** and **c** Orthogonal sections confirm that the nanorods are within the cell. Confocal microscope stacked images **d** of a live HEK 293 cell stained with Lysotracker Green identifying the location of the nanorods (Rhodamine) in relation to acidic organelles in both orthogonal sections **e** and **f**. Reprinted with permission from (36) and Macmillan Publishers Ltd. © (2003).

We have taken advantage of the ability to selectively functionalize different metal segments of metallic nanorods for self-assembly and gene delivery applications (36,67–69). For example, we selectively functionalized two segment gold–nickel nanorods with a cell targeting ligand, transferrin, on the gold segment and plasmid DNA on the nickel segment (Table II). The DNA was bound to the nickel electrostatically by suspending the nanorods in a 0.1 M solution of 3-[(2-aminoethyl)dithio] propionic acid (AEDP). The carboxylic acid terminus of the AEDP binds to the native oxide on the nickel segment resulting in primary amine end groups which are spaced by a reducible disulfide linkage. (115). Transferrin is an iron-transport protein involved in receptor-mediated endocytosis that promotes cell uptake. To confirm the presence and location of the nanorods in the transfected cells, rhodamine was also tagged to the transferrin. Spatial control over the binding of the transferrin and plasmid DNA ensured that they did not interfere with each other. SEM images and confocal microscopy showed that the nanorods were internalized by the cell and located in the cytoplasm or acidic organelles. Figure 14 shows cellular location and confirmation of transfection with the green fluorescent reporter gene. Transferrin attachment to the nanorods increased luciferase transgene expression by fourfold when compared to nanorods with plasmid DNA alone in the human embryonic kidney (HEK293) cell line. Further enhancement of nanorod uptake by cells could be also be achieved by using a magnetic field to drive the nickel portions of the nanorods towards the cell surface. When nanorods were delivered bolistically by the gene gun to the shallow subdermal layers of murine skin, a strong but transient luciferase transgene expression was detected indicating strong potential for genetic vaccination applications (36).

Multi-functional Nanorods for Vaccine Applications

Multifunctional nanorods can significantly enhance an antigen-specific immune response. In a follow-up study to the multi-component nanorods for non-viral gene delivery, we engineered gold–nickel nanorods with ovalbumin (OVA), a model protein antigen, on the gold segments and empty insert plasmids with an immunostimulatory CpG sequence on

the nickel segment. When both OVA and CpG motifs were bound to the same nanorod, we observed a tenfold increase in the CD8+ T-cell response in comparison to OVA delivery on nanorods alone (Fig. 15). In the body, antigens are taken up by antigen presenting cells, such as macrophages and dendritic cells. Antigens can be processed via class I or class II pathways. If processed via the class II pathway—which is typical for antigens alone—a strong CD8+ T-cell response is not generated. CpG motifs help to chaperone the antigen to be processed via the class I pathway by binding to toll like receptor 9 (69,116–118). The multifunctional nanorods, in this case, are critical in ensuring that both the antigen and CpG are delivered to the same cell. When the encoded antigen is tumor specific, a strong CD8+ T cell and antibody response can be generated to attack the tumor and prevent recurrence (69,115,119–121). Multifunctional nanorods, therefore, have significant potential as immunotherapeutic anti-tumor vaccines.

CONCLUSION

This review has discussed some of the key developments in multifunctional nanorods for use in biomedical applications. Depending on the synthesis method and type of functionalization, the nanorods can be used in DNA detection assays, protein and glucose sensing, targeted gene delivery, and vaccine applications. Applying these specific functionalities to different segments of the nanorods greatly increases the versatility of the system and allows for additional functionalities to be introduced for imaging, positioning, and delivery enhancement. Continued exploration into the possibilities of multifunctional nanorods could overcome previous hurdles in this exciting and convergent field of biomedical research.

ACKNOWLEDGEMENTS

We gratefully acknowledge support aided by grant number IRG-77-004-28 from the American Cancer Society and the National Science Foundation Nanoscale Exploratory Award. J. Melanko thanks the University of Iowa for a Presidential Fellowship.

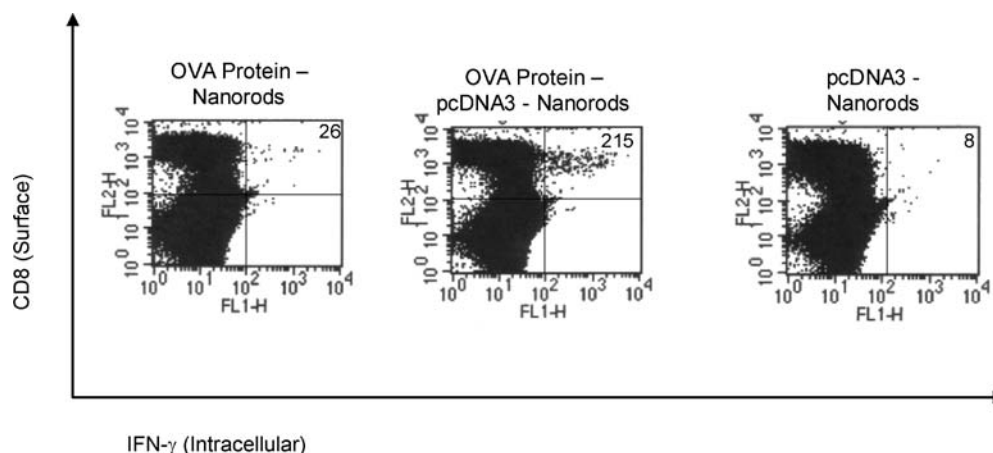


Fig. 15. Ovalbumin-specific CD8 responses in C57BL/6 mice immunized with various antigen-nanorod particle formulations. C57BL/6 mice were immunized with control blank plasmid (CpG motif) bound to nanorods, ovalbumin antigen-nanorod formulation and ovalbumin antigen/control blank pcDNA3 (CpG motif)-nanorod formulation via a gene gun. Reprinted with permission from (69). © Institute of Physics (2005).

REFERENCES

- S. Panigrahi, S. Kundu, S. K. Ghosh, S. Nath, and T. Pal. Sugar assisted evolution of mono- and bimetallic nanoparticles. *Colloids Surf., A Physicochem. Eng. Asp.* **264**:133–138 (2005).
- M. A. El-Sayed. Some interesting properties of metals confined in time and nanometer space of different shapes. *Acc. Chem. Res.* **34**:257–264 (2001).
- J. A. Creighton, C. G. Blatchford, and M. G. Albrecht. Plasma resonance enhancement of Raman scattering by pyridine adsorbed on silver or gold sol particles of size comparable to the excitation wavelength. *J. Chem. Soc. Faraday Trans.* **75**:790, 1979 (1979).
- B. Wildt, P. Mali, and P. C. Searson. Electrochemical template synthesis of multisegment nanowires: Fabrication and protein functionalization. *Langmuir* **22**:10528–10534 (2006).
- C. C. Huang, Z. Yang, and H. T. Chang. Synthesis of dumbbell-shaped Au–Ag Core-Shell nanorods by seed-mediated growth under alkaline conditions. *Langmuir* **20**:6089–6092 (2004).
- A. Henglein. Preparation and optical absorption spectra of Au-core-Pt-shell and Pt-core-Au-shell colloidal nanoparticles in aqueous solution. *J. Phys. Chem. B.* **104**:2201–2203 (2000).
- J. H. Hodak, A. Henglein, and G. V. Hartland. Coherent excitation of acoustic breathing modes in bimetallic core-shell nanoparticles. *J. Phys. Chem. B.* **104**:5053–5055 (2000).
- V. P. Torchilin. Multifunctional nanocarriers. *Adv. Drug Deliv. Rev.* **58**:1532–1555 (2006).
- S. J. Hurst, E. K. Payne, L. D. Qin, and C. A. Mirkin. Multisegmented one-dimensional nanorods prepared by hard-template synthetic methods. *Angewandte Chemie—International Edition.* **45**:2672–2692 (2006).
- L. A. Bauer, N. S. Birenbaum, and G. J. Meyer. Biological applications of high aspect ratio nanoparticles. *J. Mater. Chem.* **14**:517–526 (2004).
- I. W. Eugenii Katz. Integrated nanoparticle-biomolecule hybrid systems: Synthesis, properties, and applications. *ChemInform.* **43**, 6042–6108 (2004).
- P. C. Lee and D. Meisel. Adsorption and surface-enhanced Raman of dyes on silver and gold sols. *J. Phys. Chem.* **86**:3391–3395 (1982).
- A. Gole and C. J. Murphy. Seed-mediated synthesis of gold nanorods: Role of the size and nature of the seed. *Chem. Mater.* **16**:3633–3640 (2004).
- L. Lu, H. Wang, Y. Zhou, S. Xi, H. Zhang, and B. Zhao. Seed-mediated growth of large, monodisperse core-shell gold–silver nanoparticles with Ag-like optical properties. *Chem. Commun.* 144–145 (2002).
- L. Wang, G. Wei, L. L. Sun, Z. G. Liu, Y. H. Song, T. Yang, Y. J. Sun, C. L. Guo, and Z. Li. Self-assembly of cinnamic acid-capped gold nanoparticles. *Nanotechnology.* **17**:2907–2912 (2006).
- L. H. Pei, K. Mori, and M. Adachi. Formation process of two-dimensional networked gold nanowires by citrate reduction of AuCl₄⁻ and the shape stabilization. *Langmuir* **20**:7837–7843 (2004).
- C. J. Murphy, T. K. San, A. M. Gole, C. J. Orendorff, J. X. Gao, L. Gou, S. E. Hunyadi, and T. Li. Anisotropic metal nanoparticles: Synthesis, assembly, and optical applications. *J. Phys. Chem. B.* **109**:13857–13870 (2005).
- D. H. Qin, J. W. Zhou, C. Luo, Y. S. Liu, L. L. Han, and Y. Cao. Surfactant-assisted synthesis of size-controlled trigonal Se/Te alloy nanowires. *Nanotechnology* **17**:674–679 (2006).
- G. Glavee, K. Klabunde, C. Sorensen, and G. Hadjippanayis. Chemistry of borohydride reduction of iron(II) and iron(III) ions in aqueous and nonaqueous media—formation of nanoscale Fe, Fe₂O₃, and Fe₂B powders. *Inorg. Chem.* **34**:28–35 (1995).
- L. Longenberger and G. Mills. Formation of metal particles in aqueous solutions by reactions of metal complexes with polymers. *J. Phys. Chem.* **99**:475–478 (1995).
- S. Ayyappan, R. Srinivasa, G. N. Gopalan, and C. N. R. Subbanna. Nanoparticles of Ag, Au, Pd, and Cu produced by alcohol reduction of the salts. *J. Mater. Res.* **12**:398–401 (1997).
- Z. L. Wang, Y. Liu, Z. Zhang. *Handbook of nanophase and nanostructured materials*, Kluwer Academic Publishers, New York, 2002.
- Y. Cui, X. Duan, Y. Huang, and C. Lieber. Nanowires as Building Blocks for nanoscale Science and Technology. Nanowires and Nanobelts—Materials, Properties and Devices, Tsinghua University Press, 3–68.
- Y. Jin and S. Dong. One-pot synthesis and characterization of novel silver–gold bimetallic nanostructures with hollow interiors and bearing nanospikes. *J. Phys. Chem. B.* **107**:12902–12905 (2003).
- X. Q. Zou, E. B. Ying, and S. J. Dong. Preparation of novel silver–gold bimetallic nanostructures by seeding with silver nanoparticles and application in surface-enhanced Raman scattering. *J. Colloid Interface Sci.* **306**:307–315 (2007).
- K. S. Shankar and A. K. Raychaudhuri. Fabrication of nanowires of multicomponent oxides: Review of recent advances. *Mater. Sci. Eng. C.* **25**:738–751 (2005).
- K. Zou, X. H. Zhang, X. F. Duan, X. M. Meng, and S. K. Wu. Seed-mediated synthesis of silver nanostructures and polymer/silver nanocables by UV irradiation. *J. Cryst. Growth.* **273**:285–291 (2004).
- S. J. Hurst, E. K. Payne, L. Qin, and C. A. Mirkin. Multisegmented one-dimensional nanorods prepared by hard-template synthetic methods. *Angew. Chem. Int. Ed.* **45**:2672–2692 (2006).
- A. Blondel, B. Doudin, and J. P. Ansermet. Comparative study of the magnetoresistance of electrodeposited Co/Cu multilayered nanowires made by single and dual bath techniques. *J. Magn. Magn. Mater.* **165**:34–37 (1997).
- C. D. Keating and M. J. Natan. Striped metal nanowires as building blocks and optical tags. *Adv. Mater.* **15**:451–454 (2003).
- T. Ohgai, X. Hoffer, A. Fábán, L. Gravier, and J.-P. Ansermet. Electrochemical synthesis and magnetoresistance properties of Ni, Co and Co/Cu nanowires in a nanoporous anodic oxide layer on metallic aluminium. *J. Mater. Chem.* **13**:2530–2534 (2003).
- A. M. Asaduzzaman and M. Springborg. Structural and electronic properties of Au, Pt, and their bimetallic nanowires. *Phys. Rev. B.* **72**:2005 (2005).
- B. R. Martin, D. J. Dermody, B. D. Reiss, M. Fang, L. A. Lyon, M. J. Natan, and T. E. Mallouk. Orthogonal self-assembly on colloidal gold–platinum nanorods. *Adv. Mater.* **11**:1021–1025 (1999).
- M. Mandal, N. R. Jana, S. Kundu, S. K. Ghosh, M. Panigrahi, and T. Pal. Synthesis of Au-core–Ag-shell type bimetallic nanoparticles for single molecule detection in solution by SERS method. *J. Nanopart. Res.* **6**:53–61 (2004).
- S. R. Nicewarner-Pena, R. G. Freeman, B. D. Reiss, L. He, D. J. Pena, I. D. Walton, R. Cromer, C. D. Keating, and M. J. Natan. Submicrometer metallic barcodes. *Science.* **294**:137–141 (2001).
- A. K. Salem, P. C. Searson, and K. W. Leong. Multifunctional nanorods for gene delivery. *Nature Materials.* **2**:668–671 (2003).
- A. K. Salem. Co-delivery of antigens and adjuvants by particle bombardment of multicomponent metallic nanorods. *Abstracts of Papers of the American Chemical Society* **230**:U1201–U1202 (2005).
- F. Liu, J. Y. Lee, and W. J. Zhou. Multisegment PtRu nanorods: Electrocatalysts with adjustable bimetallic pair sites. *Adv. Funct. Mater.* **15**:1459–1464 (2005).
- D. J. Pena, J. K. N. Mbindyo, A. J. Carado, T. E. Mallouk, C. D. Keating, B. Razavi, and S. Mayer. Template growth of photoconductive metal–CdSe–metal nanowires. *J. Phys. Chem. B.* **106**:7458–7462 (2002).
- E. C. Walter, B. J. Murray, F. Favier, and R. M. Penner. “Beaded” bimetallic nanowires: Wiring nanoparticles of metal 1 using nanowires of metal 2. *Adv. Mater.* **15**:396–399 (2003).
- X. H. Liu, J. Q. Wang, J. Y. Zhang, and S. R. Yang. Fabrication and characterization of LiFePO₄ nanotubes by a sol–gel–AAO template process. *Chinese Journal of Chemical Physics* **19**:530–534 (2006).

42. X. H. Liu, J. Q. Wang, J. Y. Zhang, and S. R. Yang. Sol-gel template synthesis of LiV_3O_8 nanowires. *J. Mater. Sci.* **42**:867–871 (2007).
43. E. Braun, Y. Eichen, U. Sivan, and G. Ben-Yoseph. DNA-templated assembly and electrode attachment of a conducting silver wire. *Nature* **391**:775–778 (1998).
44. E. Gazit. Use of biomolecular templates for the fabrication of metal nanowires. *Febs Journal* **274**:317–322 (2007).
45. P. M. Harrison and P. Arosio. The ferritins: Molecular properties, iron storage function and cellular regulation. *Biochim. Biophys. Acta (BBA)—Bioenerg.* **1275**:161–203 (1996).
46. T. Douglas, D. P. E. Dickson, S. Betteridge, J. Charnock, C. D. Garner, and S. Mann. Synthesis and structure of an iron(III) sulfide-ferritin bioinorganic nanocomposite. *Science* **269**:54–57 (1995).
47. F. C. Meldrum, T. Douglas, S. Levi, P. Arosio, and S. Mann. Reconstitution of manganese oxide cores in horse spleen and recombinant ferritins. *J. Inorg. Biochem.* **58**:59–68 (1995).
48. S. M. Kim and K. W. Wong. Biomimetic synthesis of cadmium sulfide-ferritin nanocomposites. *Adv. Mater.* **8**:928–932 (1996).
49. M. Reches and E. Gazit. Casting metal nanowires within discrete self-assembled peptide nanotubes. *Science* **300**:625–627 (2003).
50. S. Padalkar, J. Hulleman, P. Deb, K. Cunzeman, J. C. Rochet, E. A. Stach, and L. Stanciu. Alpha-synuclein as a template for the synthesis of metallic nanowires. *Nanotechnology*. **18**:(2007).
51. S. J. Son and S. B. Lee. Controlled gold nanoparticle diffusion in nanotubes: Platform of partial functionalization and gold capping. *J. Am. Chem. Soc.* **128**:15974–15975 (2006).
52. B. R. Martin, D. J. Dermody, B. D. Reiss, M. Fang, L. A. Lyon, M. J. Natan, and T. E. Mallouk. Orthogonal self-assembly on colloidal gold-platinum nanorods. *Adv. Mater.* **11**:1021–1025 (1999).
53. X. J. Wu, W. An, and X. C. Zeng. Chemical functionalization of boron-nitride nanotubes with NH_3 and amino functional groups. *J. Am. Chem. Soc.* **128**:12001–12006 (2006).
54. M. Nakanishi, H. Takatani, Y. Kobayashi, F. Hori, R. Taniguchi, A. Iwase, and R. Oshima. Characterization of binary gold/platinum nanoparticles prepared by sonochemistry technique. *Appl. Surf. Sci.* **241**:209–212 (2005).
55. Y. Mizukoshi, T. Fujimoto, Y. Nagata, R. Oshima, and Y. Maeda. Characterization and catalytic activity of core-shell structured gold/palladium bimetallic nanoparticles synthesized by the sonochemical method. *J. Phys. Chem. B.* **104**:6028–6032 (2000).
56. H. Takatani, H. Kago, M. Nakanishi, Y. Kobayashi, F. Hori, and R. Oshima. Characterization of noble metal alloy nanoparticles prepared by ultrasound irradiation. *Rev. Adv. Mater. Sci.* **5**:232–238 (2003).
57. N. S. Birenbaum, B. T. Lai, C. S. Chen, D. H. Reich, and G. J. Meyer. Selective noncovalent adsorption of protein to bifunctional metallic nanowire surfaces. *Langmuir* **19**:9580–9582 (2003).
58. D. T. Mitchell, S. B. Lee, L. Trofin, N. Li, T. K. Nevanen, H. Soderlund, and C. R. Martin. Smart nanotubes for bioseparations and biocatalysis. *J. Am. Chem. Soc.* **124**:11864–11865 (2002).
59. J. K. N. Mbindyo, T. E. Mallouk, J. B. Mattzela, I. Kratochvilova, B. Razavi, T. N. Jackson, and T. S. Mayer. Template synthesis of metal nanowires containing monolayer molecular junctions. *J. Am. Chem. Soc.* **124**:4020–4026 (2002).
60. T. F. Otero and E. Delarreta. Electrochemical control of the morphology, adherence, appearance and growth of polypyrrole films. *Synth. Met.* **26**:79–88 (1988).
61. R. M. Hernández, L. Richter, S. Semancik, S. Stranick, and T. E. Mallouk. Template fabrication of protein-functionalized gold-polypyrrole-gold segmented nanowires. *Chem. Mater.* **16**:3431–3438 (2004).
62. S. Wang, N. Mamedova, N. A. Kotov, W. Chen, and J. Studer. Antigen/antibody immunocomplex from CdTe nanoparticle bioconjugates. *Nano Lett.* **2**:817–822 (2002).
63. Y. Eichen, E. Braun, U. Sivan, and G. Ben-Yoseph. Self-assembly of nanoelectronic components and circuits using biological templates. *Acta Polym.* **49**:663–670 (1998).
64. H. Mattoussi, J. M. Mauro, E. R. Goldman, G. P. Anderson, V. C. Sundar, F. V. Mikulec, and M. G. Bawendi. Self-assembly of CdSe-ZnS Quantum Dot bioconjugates using an engineered recombinant protein. *J. Am. Chem. Soc.* **122**:12142–12150 (2000).
65. H. Matsui, P. Porrata, and G. E. Doublerly. Protein tubule immobilization on self-assembled monolayers on Au substrates. *Nano Lett.* **1**:461–464 (2001).
66. I. A. Banerjee, L. T. Yu, and H. Matsui. Location-specific biological functionalization on nanotubes: Attachment of proteins at the ends of nanotubes using Au nanocrystal masks. *Nano Lett.* **3**:283–287 (2003).
67. A. K. Salem, J. Chao, K. W. Leong, and P. C. Searson. Receptor-mediated self-assembly of multi-component magnetic nanowires. *Adv. Mater.* **16**:268–271 (2004).
68. A. K. Salem, M. Chen, J. Hayden, K. W. Leong, and P. C. Searson. Directed assembly of multisegment Au/Pt/Au nanowires. *Nano Lett.* **4**:1163–1165 (2004).
69. A. K. Salem, C. F. Hung, T. W. Kim, T. C. Wu, C. Searson, and K. W. Leong. Multi-component nanorods for vaccination applications. *Nanotechnology* **16**:484–487 (2005).
70. L. Soon, F. Braet, and J. Condeelis. Moving in the right direction—Nanoimaging in cancer cell motility and metastasis. *Microsc. Res. Tech.* **70**:252–257 (2007).
71. Y. W. C. Cao, R. C. Jin, and C. A. Mirkin. Nanoparticles with Raman spectroscopic fingerprints for DNA and RNA detection. *Science* **297**:1536–1540 (2002).
72. B. J. Battersby, D. Bryant, W. Meuterms, D. Matthews, M. L. Smythe, and M. Trau. Toward larger chemical libraries: Encoding with fluorescent colloids in combinatorial chemistry. *J. Am. Chem. Soc.* **122**:2138–2139 (2000).
73. J. Ni, R. J. Lipert, G. B. Dawson, and M. D. Porter. Immunoassay readout method using extrinsic Raman labels adsorbed on immunogold colloids. *Anal. Chem.* **71**:4903–4908 (1999).
74. S. A. Dunbar and J. W. Jacobson. Application of the Luminex LabMAP in rapid screening for mutations in the cystic fibrosis transmembrane conductance regulator gene: A pilot study. *Clin. Chem.* **46**:1498–1500 (2000).
75. M. Y. Han, X. H. Gao, J. Z. Su, and S. Nie. Quantum-dot-tagged microbeads for multiplexed optical coding of biomolecules. *Nat. Biotechnol.* **19**:631–635 (2001).
76. D. R. Walt. Molecular biology—Bead-based fiber-optic arrays. *Science* **287**:451–452 (2000).
77. J. B. H. Tok, F. Y. S. Chuang, M. C. Kao, K. A. Rose, S. S. Pannu, M. Y. Sha, G. Chakarova, S. G. Penn, and G. M. Dougherty. Metallic striped nanowires as multiplexed immunoassay platforms for pathogen detection. *Angew. Chem.—Int. Ed.* **45**:6900–6904 (2006).
78. D. C. Pregibon, M. Toner, and P. S. Doyle. Multifunctional encoded particles for high-throughput biomolecule analysis. *Science* **315**:1393–1396 (2007).
79. P. Alivisatos. The use of nanocrystals in biological detection. *Nat. Biotechnol.* **22**:47–52 (2004).
80. J. Kong, N. R. Franklin, C. Zhou, M. G. Chapline, S. Peng, K. Cho, and H. Dai. Nanotube molecular wires as chemical sensors. *Science* **287**:622–625 (2000).
81. A. M. Fond, N. S. Birenbaum, E. J. Felton, D. H. Reich, and G. J. Meyer. Preferential noncovalent immunoglobulin G adsorption onto hydrophobic segments of multi-functional metallic nanowires. *J. Photochem. Photobiol. A: Chem.* **186**:57–64 (2007).
82. J. T. Sheu, C. C. Chen, P. C. Huang, Y. K. Lee, and M. L. Hsu. Selective deposition of gold nanoparticles on SiO_2/Si nanowires for molecule detection. *Jpn. J. Appl. Phys. Part 1—Regular Papers Short Notes & Review Papers.* **44**:2864–2867 (2005).
83. NIH. Diabetes. *NIH MedlinePlus Medical Encyclopedia*, U.S. National Library of Medicine and National Institutes of Health (2005).

84. J. Wang and M. Musameh. Carbon nanotube/teflon composite electrochemical sensors and biosensors. *Anal. Chem.* **75**:2075–2079 (2003).
85. B. R. Azamian, J. J. Davis, K. S. Coleman, C. B. Bagshaw, and M. L. H. Green. Bioelectrochemical single-walled carbon nanotubes. *J. Am. Chem. Soc.* **124**:12664–12665 (2002).
86. K. Besteman, J. O. Lee, F. G. M. Wiertz, H. A. Heering, and C. Dekker. Enzyme-coated carbon nanotubes as single-molecule biosensors. *Nano Lett.* **3**:727–730 (2003).
87. K. S. Lee and M. A. El-Sayed. Gold and silver nanoparticles in sensing and imaging: Sensitivity of plasmon response to size, shape, and metal composition. *J. Phys. Chem. B.* **110**:19220–19225 (2006).
88. C. P. T. Svensson, W. Seifert, M. W. Larsson, L. R. Wallenberg, J. Stangl, G. Bauer, and L. Samuelson. Epitaxially grown GaP/GaAs_{1-x}P_x/GaP double heterostructure nanowires for optical applications. *Nanotechnology* **16**:936–939 (2005).
89. M. H. Huang, S. Mao, H. Feick, H. Q. Yan, Y. Y. Wu, H. Kind, E. Weber, R. Russo, and P. D. Yang. Room-temperature ultraviolet nanowire nanolasers. *Science.* **292**:1897–1899 (2001).
90. I. Gur, N. A. Fromer, M. L. Geier, and A. P. Alivisatos. Air-stable all-inorganic nanocrystal solar cells processed from solution. *Science* **310**:462–465 (2005).
91. A. L. Pan, H. Yang, R. B. Liu, R. C. Yu, B. S. Zou, and Z. L. Wang. Color-tunable photoluminescence of alloyed CdS_xSe_{1-x} nanobelts. *J. Am. Chem. Soc.* **127**:15692–15693 (2005).
92. X. G. Peng, L. Manna, W. D. Yang, J. Wickham, E. Scher, A. Kadavanich, and A. P. Alivisatos. Shape control of CdSe nanocrystals. *Nature* **404**:59–61 (2000).
93. Z. A. Peng and X. G. Peng. Mechanisms of the shape evolution of CdSe nanocrystals. *J. Am. Chem. Soc.* **123**:1389–1395 (2001).
94. X. G. Peng. Mechanisms for the shape-control and shape-evolution of colloidal semiconductor nanocrystals. *Adv. Mater.* **15**:459–463 (2003).
95. T. Kuykendall, P. J. Pauzauskie, Y. F. Zhang, J. Goldberger, D. Sirbulu, J. Denlinger, and P. D. Yang. Crystallographic alignment of high-density gallium nitride nanowire arrays. *Nature Materials* **3**:524–528 (2004).
96. J. Goldberger, R. R. He, Y. F. Zhang, S. W. Lee, H. Q. Yan, H. J. Choi, P. D. Yang. Single-crystal gallium nitride nanotubes. *Nature.* **422**:599–602 (2003).
97. G. S. Yi, H. C. Lu, S. Y. Zhao, G. Yue, W. J. Yang, D. P. Chen, and L. H. Guo. Synthesis, characterization, and biological application of size-controlled nanocrystalline NaYF₄ : Yb,Er infrared-to-visible up-conversion phosphors. *Nano Lett.* **4**:2191–2196 (2004).
98. F. van de Rijke, H. Zijlmans, S. Li, T. Vail, A. K. Raap, R. S. Niedbala, and H. J. Tanke. Up-converting phosphor reporters for nucleic acid microarrays. *Nat. Biotechnol.* **19**:273–276 (2001).
99. L. Y. Wang, R. X. Yan, Z. Y. Hao, L. Wang, J. H. Zeng, H. Bao, X. Wang, Q. Peng, and Y. D. Li. Fluorescence resonant energy transfer biosensor based on upconversion-luminescent nanoparticles. *Angew. Chem.—Int. Ed.* **44**:6054–6057 (2005).
100. J. H. Zeng, J. Su, Z. H. Li, R. X. Yan, and Y. D. Li. Synthesis and upconversion luminescence of hexagonal-phase NaYF₄ : Yb, Er³⁺, phosphors of controlled size and morphology. *Adv. Mater.* **17**:2119–2123 (2005).
101. S. Heer, K. Kompe, H. U. Gudel, and M. Haase. Highly efficient multicolor upconversion emission in transparent colloids of lanthanide-doped NaYF₄ nanocrystals. *Adv. Mater.* **16**:2102–+ (2004).
102. X. Wang, J. Zhuang, Q. Peng, and Y. D. Li. A general strategy for nanocrystal synthesis. *Nature* **437**:121–124 (2005).
103. L. Y. Wang and Y. D. Li. Na(Y_{1.5}Na_{0.5})F₆ single-crystal nanorods as multicolor luminescent materials. *Nano Lett.* **6**:1645–1649 (2006).
104. A. P. Alivisatos. Semiconductor clusters, nanocrystals, and quantum dots. *Science* **271**:933–937 (1996).
105. J. Janata and M. Josowicz. Conducting polymers in electronic chemical sensors. *Nature Materials* **2**:19–24 (2003).
106. A. K. Wanekaya, W. Chen, N. V. Myung, and A. Mulchandani. Nanowire-based electrochemical biosensors. *Electroanalysis* **18**:533–550 (2006).
107. H. Chik, J. Liang, S. G. Cloutier, N. Kouklin, and J. M. Xu. Periodic array of uniform ZnO nanorods by second-order self-assembly. *Appl. Phys. Lett.* **84**:3376–3378 (2004).
108. B. J. Taft, A. D. Lazareck, G. D. Withey, A. J. Yin, J. M. Xu, and S. O. Kelley. Site-specific assembly of DNA and appended cargo on arrayed carbon nanotubes. *J. Am. Chem. Soc.* **126**:12750–12751 (2004).
109. Q. Ren, Y. P. Zhao, J. C. Yue, and Y. B. Cui. Biological application of multi-component nanowires in hybrid devices powered by F-1-ATPase motors. *Biomedical Microdevices* **8**:201–208 (2006).
110. D. Cai, J. M. Mataraza, Z. H. Qin, Z. P. Huang, J. Y. Huang, T. C. Chiles, D. Carnahan, K. Kempa, and Z. F. Ren. Highly efficient molecular delivery into mammalian cells using carbon nanotube sparring. *Nature Methods.* **2**:449–454 (2005).
111. D. Pantarotto, R. Singh, D. McCarthy, M. Erhardt, J. P. Briand, M. Prato, K. Kostarelos, and A. Bianco. Functionalized carbon nanotubes for plasmid DNA gene delivery. *Angew. Chem.—Int. Ed.* **43**:5242–5246 (2004).
112. A. A. Wang, J. Lee, G. Jenikova, A. Mulchandani, N. V. Myung, and W. Chen. Controlled assembly of multi-segment nanowires by histidine-tagged peptides. *Nanotechnology* **17**:3375–3379 (2006).
113. A. Vogel and V. Venugopalan. Mechanisms of pulsed laser ablation of biological tissues (vol 103, pg 577, 2003). *Chem. Rev.* **103**:2079–2079 (2003).
114. R. Weissleder. A clearer vision for *in vivo* imaging. *Nat. Biotechnol.* **19**:316–317 (2001).
115. A. K. Salem, P. C. Searson, and K. W. Leong. Multifunctional nanorods for gene delivery. *Nature Materials* **2**:668–671 (2003).
116. A. K. Salem, A. D. Sandler, G. J. Weiner, X. Q. Zhang, N. K. Baman, X. Zhu, and C. E. Dahle. Immunostimulatory antigen loaded microparticles as cancer vaccines. *Molec. Ther.* (2006).
117. X. Q. Zhang, C. E. Dahle, G. J. Weiner, and A. K. Salem. A comparative study of the antigen-specific immune response induced by co-delivery of CpG ODN and antigen using fusion molecules or biodegradable microparticles. *J. Pharm. Sci.* In press DOI 10.1002/jps.20978 (2007).
118. X. Q. Zhang, C. E. Dahle, N. K. Baman, N. Rich, G. J. Weiner, and A. K. Salem. Potent antigen-specific immune responses stimulated by co-delivery of CpG ODN and antigens in degradable microparticles. *J. Immunother.* **30**(5):469–478 (2007).
119. C. F. Hung and T. C. Wu. Improving DNA vaccine potency via modification of professional antigen presenting cells. *Curr. Opin. Mol. Ther.* **5**:20–24 (2003).
120. C. F. Hung, W. F. Cheng, K. F. Hsu, C. Y. Chai, L. M. He, M. Ling, and T. C. Wu. Cancer immunotherapy using a DNA vaccine encoding the translocation domain of a bacterial toxin linked to a tumor antigen. *Cancer Res.* **61**:3698–3703 (2001).
121. S. Raychaudhuri and K. L. Rock. Fully mobilizing host defense: Building better vaccines. *Nat. Biotechnol.* **16**:1025–1031 (1998).
122. L. L. Zhao, T. Z. Lu, M. Yosef, M. Steinhart, M. Zacharias, U. Gosele, and S. Schlecht. Single-crystalline CdSe nanostructures: From primary grains to oriented nanowires. *Chem. Mater.* **18**:6094–6096 (2006).
123. A. D. Lazareck, T. F. Kuo, J. M. Xu, B. J. Taft, S. O. Kelley, and S. G. Cloutier. Optoelectrical characteristics of individual zinc oxide nanorods grown by DNA directed assembly on vertically aligned carbon nanotube tips. *Appl. Phys. Lett.* **89**:(2006).
124. Y. Xia, P. Yang, Y. Sun, Y. Wu, B. Mayers, B. Gates, Y. Yin, F. Kim, and H. Yan. One-dimensional nanostructures: Synthesis, characterization, and applications. *Adv. Mater.* **15**:353–389 (2003).
125. L. J. Lauhon, M. S. Gudiksen, D. Wang, and C. M. Lieber. Epitaxial core-shell and core-multishell nanowire heterostructures. *Nature* **420**:57–61 (2002).